Sources and fate of nitrate in groundwater at agricultural operations overlying glacial sediments

Sarah A. Bourke[1,2], Mike Iwanyshyn[3], Jacqueline Kohn[4], M. Jim Hendry[1]

[1]Department of Geological Sciences, University of Saskatchewan, SK, S7N 5C9, Canada
[2]School of Earth Sciences, University of Western Australia, Crawley, WA, 6009, Australia
[3]Natural Resources Conservation Board, Calgary, AB, T2P 0R4, Canada
[4]Alberta Agriculture and Forestry, Irrigation and Farm Water Branch, Edmonton, AB, T6H 5T6, Canada

Correspondence to: Sarah A. Bourke (sarah.bourke@uwa.edu.au)

Abstract. Leaching of nitrate (NO_3^-) from animal waste or fertilizers at agricultural operations can result in NO_3^- contamination of groundwater, lakes, and streams. Understanding the sources and fate of nitrate in groundwater systems in glacial sediments, which underlie many agricultural operations, is critical for managing impacts of human food production on the environment. Elevated NO_3^- concentrations in groundwater can be naturally attenuated through mixing or denitrification. Here we use isotopic enrichment of the stable isotope values of NO_3^- to quantify the amount of denitrification in groundwater at two confined feeding operations overlying glacial sediments in Alberta, Canada. Uncertainty in $\delta^{15}N_{NO3}$ and $\delta^{18}O_{NO3}$ values of the NO_3^- source and denitrification enrichment factors are accounted for using a Monte Carlo approach. When denitrification could be quantified, we used these values to constrain a mixing model based on NO_3^- and Cl^- concentrations. Using this novel approach we were able to reconstruct the initial NO_3-N concentration and NO_3-N/Cl^- ratio at the point of entry to the groundwater system. The addition of NO_3^- to the local groundwater system from temporary manure piles and pens equalled or exceeded NO_3^- additions due to leaching from earthen manure storages at these sites. As such, on-farm management of manure waste to limit NO_3^- contamination of groundwater should increasingly focus on limiting manure piles in direct contact with the soil, and encourage storage in lined lagoons. Nitrate attenuation at both sites is attributed to a spatially variable combination of mixing and denitrification, but is dominated by denitrification. On-site denitrification reduced agriculturally derived NO_3^- concentrations by at least half and, in some wells, completely. Therefore, infiltration to groundwater systems in glacial sediments where NO_3^- can be naturally attenuated is likely preferable to off-farm export via runoff or drainage networks, if local groundwater is not used for potable water supply.

1 Introduction

The contamination of soil and groundwater with nitrate from agricultural operations is a global water quality issue that has been extensively documented (Power and Schepers, 1989; Spalding and Exner, 1993; Rodvang and Simpkins, 2001; Galloway et al., 2008; Zirkle et al., 2016; Arauzo, 2017; Ascott et al., 2017). Leaching of nitrate (NO_3^-) from animal waste or fertilizers can result in groundwater NO_3^- concentrations that exceed drinking water guidelines and pose human health risks (Fan and Steinberg, 1996; Gulis et al., 2002; Yang et al., 2007). The discharge of high-NO_3^- groundwater, runoff, or drainage can contaminate streams and lakes, resulting in eutrophication and ecosystem decline (Deutsch et al., 2006; Kaushal et al., 2011). In saturated groundwater

systems with low oxygen concentrations, elevated NO_3^- can be naturally attenuated by microbial denitrification (Wassenaar, 1995; Robertson et al., 1996; Smith et al., 1996; Tesoriero et al., 2000; Singleton et al., 2007). Concentrations of NO_3^- will also decrease along groundwater flow paths due to attenuation via dilution by hydrodynamic dispersion (referred to hereafter as mixing). Because of these natural attenuation mechanisms, infiltration to groundwater may be preferable to off-site drainage and runoff of nitrate-rich waters. Many agricultural operations are undertaken on fertile soils associated with glacial sediments (Spalding and Exner, 1993; Ernstsen et al., 2015; Zirkle et al., 2016). Understanding the sources and fate of agriculturally derived nitrate in groundwater systems in glacial sediments is therefore critical for managing impacts of human food production on the environment.

Identification of the sources and fate of NO_3^- at agricultural operations can be challenging because of spatial and temporal variations in sources (e.g. earthen manure storage, temporary manure piles, or fertilizer) and the complexity of hydrogeologic systems (Spalding and Exner, 1993; Rodvang et al., 2004; Showers et al., 2008; Kohn et al., 2016). These spatial and temporal variations can result in complex subsurface solute distributions that are difficult to interpret using classical transect studies or numerical groundwater models (Green et al., 2010; Baily et al., 2011).

Groundwater containing significant agriculturally derived NO_3^- also typically has elevated chloride (Cl^-) concentrations (Saffigna and Keeney, 1977; Rodvang et al., 2004; Menció et al., 2016). Decreasing NO_3-N/Cl^- (or NO_3^-/Cl^-) ratios have been used to define denitrification based on the assumption that NO_3^- is reactive while Cl^- is non-reactive (conservative), such that denitrification results in a decrease in the NO_3-N/Cl^- ratio (Kimble et al., 1972; Weil et al., 1990; Liu et al., 2006; McCallum et al., 2008). However, NO_3-N/Cl^- ratios can also change in response to mixing of groundwater with different NO_3-N/Cl^- ratios or when groundwater sampling traverses hydraulically disconnected formations (Bourke et al., 2015b). If NO_3-N/Cl^- ratios vary among potential sources and the NO_3-N/Cl^- ratio at the point of entry to the groundwater system can be reconstructed, this information could be used to show that anthropogenic NO_3^- at different locations within an aquifer is derived from the same or different sources.

The stable isotopes of NO_3^- ($\delta^{15}N_{NO3}$ and $\delta^{18}O_{NO3}$) provide an alternative approach to characterize the source and fate of NO_3^- in groundwater systems. In agricultural areas, multiple sources of NO_3^- are common and could include precipitation, soil NO_3^-, inorganic fertilizer, manure, and septic waste (Komor and Anderson, 1993; Liu et al., 2006; Pastén-Zapata et al., 2014; Clague et al., 2015; Xu et al., 2015). While source identification is theoretically possible using $\delta^{15}N_{NO3}$ and $\delta^{18}O_{NO3}$ (particularly with a dual-isotope approach), in practice this can be difficult due to geologic heterogeneity, overlapping source values, and the complexity of biologically mediated reactions (Aravena et al., 1993; Wassenaar, 1995; Mengis et al., 2001; Choi et al., 2003; Granger et al., 2008; Vavilin and Rytov, 2015; Xu et al., 2015). NO_3^- attenuation by denitrification in groundwater systems can be identified based on the characteristic enrichment of $\delta^{15}N_{NO3}$ and $\delta^{18}O_{NO3}$. Numerous studies have made qualitative assessments that identified denitrification in groundwater using the stable isotope approach (Böttcher et al., 1990; Wassenaar, 1995; Singleton et al., 2007; Baily et al., 2011; Clague et al., 2015; Xu et al., 2015). Recently published papers have also used stable isotopic values of NO_3^- and water as the basis for mixing models in agricultural settings (Ji et al., 2017 ;Lentz and Lehersch, 2019). Isotopic fractionation effects can also allow for quantitative assessment of the proportion of substrate that has undergone a given reaction, if enrichment factors and source values are known; as in the case of evpoarative loss of water, for example (Dogramaci et al., 2012). To date, there have been

very few attempts to quantify denitrification using dual-isotope enrichment, largely due to uncertainty in source values and enrichment factors (Böttcher et al., 1990, Xue et al., 2009).

The only published calculations of the fraction of NO_3^- remaining after denitrification the that we are aware of assumed a constant enrichment factor and the same isotopic source values across the field site (Otero et al., 2009).

5   However, the enrichment factor will vary across a field site in response to reaction rates (Kendall and Aravena 2000), and isotopic values of even the same type of source (e.g. manure) can vary substantially (Xue et al., 2009). If the varation in source values and enrichment factors can be characterized from measured data then these uncertainties can be accounted for using a Monte Carlo approach (Joerin et al., 2002; Bourke et al., 2015a; Ji et al., 2017), thereby extending the application of the dual-isotope technique to allow for a robust quantitative

10   assessment of denitrification in agricultural settings.

A synthesized analysis of stable isotopes of NO_3^- with additional ionic tracers can further improve the assessment of NO_3^- attenuation mechanisms and sources of NO_3^- in agricultural settings (Showers et al., 2008; Vitòria et al., 2008; Xue et al., 2009; Xu et al., 2015; Ji et al., 2017). We hypothesise that if the amount of denitrification can be quantified based on $\delta^{15}N_{NO3}$ and $\delta^{18}O_{NO3}$, then this estimate of the fraction of NO_3-N removed through

15   denitrification can be used to constrain a mixing model based on NO_3-N and Cl^- concentrations. This novel approach allows for the ratio of NO_3-N/Cl^- at the point of entry to the groundwater system to be reconstructed from measured NO_3^- and Cl^- concentrations (see Section 2.3). Where the NO_3-N/Cl^- ratio varies between sources, this ratio can then be used to assess the source of the NO_3^- in groundwater (e.g. temporary manure piles or feeding pens). These data can also then be used to estimate the initial concentrations of NO_3^- and Cl^- at the point of entry

20   to the groundwater system and quantify attenuation by mixing.

In this study, we present the application of this approach at two confined feeding operations (CFOs) in Alberta, Canada, with differing lithologies and durations of operation (Fig. 1). Concentrations of Cl^- and nitrogen species (N-species) and the stable isotopes of NO_3^- were measured in groundwater samples collected from monitoring wells and continuous soil cores, as well as manure filtrate at both sites. These data were interpreted to (1) assess

25   the extent of agriculturally derived NO_3^- in groundwater, (2) identify sources and initial concentrations of NO_3^- at the point of entry to the groundwater system, and (3) assess the dominant attenuation mechanisms controlling subsurface NO_3^- distributions at these sites.

2 Materials and methods

2.1 Experimental sites

30   This study was conducted using data from two of the five sites investigated by Alberta Agriculture and Forestry during an assessment of the impacts of livestock manure on groundwater quality (Lorenz et al., 2014). To the best of our knowledge (including discussions with farm operators) fertilizers have not been applied at either of these sites. As such, manure waste from livestock is assumed to be the sole source of agricultural nitrogen (N) and elevated NO_3^- concentrations in groundwater at these sites.

35   The first study site (CFO1) is located 25 km northeast of Lethbridge, Alberta (Fig. 1). Agricultural operations at this site were initiated with the construction of a dairy in 1928, with the capacity for the150 dairy cattle since the 1960s. A feedlot for beef cattle was added in 1960s along with an earthen manure storage (EMS) facility for storing liquid dairy manure (approx. 4 m deep) and a catch-basin that receives surface water runoff. This feedlot

was expanded in the 1980s to the 2000 head capacity it was at the time of this study. There is also a dugout (or slough, a shallow wetland) on site that receives local runoff and an irrigation drainage canal at the southern boundary of the property.

The second study site (CFO4) is located approximately 30 km north of Red Deer, Alberta and 300 km north of CFO1. This dairy and associated EMS (approx. 6 m deep) were constructed in 1995 and the facility had 350 head of dairy cattle at the time of the study. Runoff will drain either to the small dugout in the north-west of the site, or the natural drainage features (ephemeral ponds or a creek approx. 1.5 km east).

2.2 Sampling and instrumentation

2.2.1 Groundwater monitoring wells

Groundwater samples were collected from water table wells and piezometers (hereafter both are referred to as wells) installed at both sites (Table 1). At CFO1, groundwater samples were collected from six individual water table wells (DMW1, DMW2, DMW3, DMW4, DMW5, DMW6) and eight sets of nested wells with one well screened at the water table and one well screened 20 m below ground (BG) (DP10-2 and DP10-1, DMW10 and DP11-10b, DMW11 and DP11-11b, DMW12 and DP11-12b, DMW13 and DP11-13b, DMW14 and DP11-14b, DMW15 and DP11-15b, and DMW16 and DP11-16b). Wells DP10-2 and DP10-1 were located directly adjacent to the EMS on the hydraulically downgradient side. At CFO4, groundwater samples were collected from eight water table wells (BC1, BC2, BC3, BC4, BC5, BMW1, BMW3, BMW7) and four sets of nested wells, with wells screened across the water table and at 15 m BG. Two of these nests were located adjacent to the EMS (BMW2 and BP10-15e, BMW4 and BP10-15w) and two were hydraulically downgradient of the EMS (BMW5 and BP5-15, BMW6 and BP6-15).

Groundwater samples were collected for ion analysis (Cl⁻ and N species) quarterly between April 2010 and August 2015. All water samples were collected using a bailer after purging (1–3 casing volumes) and stored at ≤ 4 °C prior to analysis. Samples for $\delta^{15}N_{NO3}$ and $\delta^{18}O_{NO3}$ were collected from wells at CFO1 on 1 January 2013 and 1 May 2013. Samples for $\delta^{15}N_{NO3}$ and $\delta^{18}O_{NO3}$ at CFO4 were collected on 27 October 2014. Wells were purged prior to sample collection (1–3 casing volumes), and samples filtered into high-density polyethylene (HDPE) bottles in the field and frozen until analysis.

Hydraulic heads in monitoring wells were determined using manual measurements (approximately monthly, 2010-2015). Rising head response tests (slug or bail tests) were conducted to determine hydraulic conductivity (K) of the formation media surrounding the intake zone on the majority of the wells at the sites.

2.2.2 Continuous core

Continuous core was collected at CFO1 immediately adjacent to well DP11-13b on 1 May 2013 (Fig. 1). Additional core samples were collected from 1 to 5 June 2015 along a transect hydraulically downgradient of the southeastern side of the EMS at CFO1 where hydrochemistry data suggested leakage from the EMS (see Section 3). During this 2015 drilling campaign, core samples were collected at four locations (DC15-20, DC15-21, DC15-22, DC15-23) to depths of up to 15 m below surface and distances of up to 100 m from the EMS between wells DMW3 and DP11-14.

Continuous core samples were retrieved using a hollow stem auger (1.5-m core lengths) with 0.3-m sub-samples collected at approximately 1-m intervals ensuring that visually consistent lithology could be sampled. Core

samples for Cl⁻ were stored in Ziploc™ bags and kept cool until analysis. Core samples for N-species analysis were stored in Ziploc bags filled with an atmosphere of argon (99.9% Ar) to minimize oxidation and kept cool until analysis. Subsamples of each core (250-300 g) were placed under 50 MPa pressure in a Carver Series NE mechanical press with a 0.5-μm filter placed at the base of the squeezing chamber, which was placed within an Ar atmosphere to minimize oxidation. A syringe was attached to the base of the apparatus and 15 mL of filtered pore water were collected for analyses within 3.5 to 6.0 h (Hendry et al., 2013).

2.2.3 Liquid manure storages

Samples of liquid manure slurry were collected directly from the EMS at both sites and the catch basin (containing local runoff from the feedlot) at CFO1 using a pipe and plunger apparatus to sample from approximately 0.5 m below the surface. The slurry collected was subsequently filtered (0.45 μm) to separate the liquid and solid components. The water filtered from samples collected from the EMS or catch basin is hereafter referred to as manure filtrate.

2.3 Laboratory analysis

For groundwater samples from wells and manure filtrate, concentrations of Cl⁻ were determined using potentiometric titration of H_2O, with a detection limit of 5.0 mg L^{-1} and accuracy of 5% (APHA 4500-Cl⁻ D). Concentrations of NH_3 as N (NH_3-N), NO_3^- as N (NO_3-N), and NO_2^- as N (NO_2-N) in groundwater samples from wells and manure filtrate were measured by air-segmented continuous flow analysis (APHA 4500-NH3 G, APHA 4500-NO3- F). Total nitrogen (TN) was determined by high temperature catalytic combustion and chemiluminescence detection using a Shimadzu TOC-V with attached TN unit (ASTM D8083-16). Total organic nitrogen (TON) was calculated by subtracting NH_3-N, NO_3-N and NO_2-N from TN. Bicarbonate (HCO_3^-) was analyzed by titration (APHA 2320 B). Dissolved organic carbon (DOC) was analyzed by a combustion infrared method (APHA 5310 B) using a Shimadzu TOC-V system.

Pore-water samples squeezed from continuous core were analyzed for Cl⁻, NO_3-N, and NO_2-N using a Dionex IC25 ion chromatograph (IC) coupled to a Dionex As50 autosampler (EPA Method 300.1, accuracy and precision of 5.0%) (Hautman and Munch, 1997). Ammonia as N (NH_3-N) was measured by Exova Laboratories using the automated phenate method (APHA Standard 4500-NH3 G, detection limit of 0.025 mg L^{-1}, accuracy of 2% of the measured concentration, and a precision of 5% of the measured concentration).

$\delta^{15}N_{NO3}$ and $\delta^{18}O_{NO3}$ in groundwater samples (from wells and pore water from continuous core) and manure filtrate were measured at the University of Calgary (Calgary, Alberta) using the denitrifier method (Sigman et al., 2001) with an accuracy and precision of 0.3‰ for $\delta^{15}N_{NO3}$ and 0.3‰ for $\delta^{18}O_{NO3}$. Groundwater samples collected for NO_3^- isotope analysis in January 2013 were also analyzed for NO_3-N by the University of Calgary (denitrifier technique, Delta+XL).

2.4 Modelling approach

2.4.1 Quantification of denitrification based on $\delta^{15}N_{NO3}$ and $\delta^{18}O_{NO3}$

Nitrate in groundwater that has undergone denitrification is commonly reported as being identified by enrichment of $\delta^{15}N_{NO3}$ and $\delta^{18}O_{NO3}$ with a slope of about 0.5 on a cross-plot (Clark and Fritz, 1997). However, published studies of denitrification in groundwater report slopes of up to 0.77 (Mengis et al., 1999; Fukada et al., 2003;

Singleton et al., 2007). The relationship between isotopic enrichment of $\delta^{15}N_{NO3}$ and $\delta^{18}O_{NO3}$ and the fraction of NO_3-N remaining during denitrification can be described by a Rayleigh equation:

$$R = R_0 f_d^{(\frac{1}{\beta}-1)}, \tag{1}$$

where R_0 is the initial isotope ratio of the NO_3^- ($\delta^{18}O_{NO3}$ or $\delta^{15}N_{NO3}$), R is the isotopic ratio when fraction f_d of NO_3^- remains, and β is the kinetic fractionation factor (> 1) (Böttcher et al., 1990; Clark and Fritz, 1997; Otero et al., 2009; Xue et al., 2009). Kinetic fraction effects are commonly also expressed as the enrichment factor, $\varepsilon = 1000(\beta-1)$. In the case of a constant enrichment factor, f_d can be calculated from:

$$f_d = exp\left(\frac{R-R_0}{\varepsilon}\right), \tag{2}$$

and the fraction of NO_3-N removed from groundwater through denitrification is given by ($1-f_d$). The concentration of NO_3-N that would have been measured if mixing was the only attenuation mechanism (NO_3-N_{mix}) can also be calculated by dividing the measured concentration by f_d.

A sub-set of 20 samples with isotopic values of NO_3^- indicative of denitrification were identified, and for each of these samples f_d (mean and standard deviation) was calculated from Eq. (2) using a Monte Carlo approach with 500 realizations. The value of R was given by the measured isotopic ratio for each sample ($\delta^{18}O_{NO3}$ or $\delta^{15}N_{NO3}$). R_0 was allowed to vary randomly within a range of values determined from measured data and literature values. If the initial $\delta^{15}N_{NO3}$ is known, ε for $\delta^{15}N_{NO3}$ (ε_{15N}) can be determined from the slope of the linear regression line on a plot of $ln(f_d)$ vs. $\delta^{15}N_{NO3}$ (Böttcher et al., 1990). If the initial $\delta^{15}N_{NO3}$ and f_d are not known, as is the case here, ε_{15N} can be determined from the slope of the regression line on a plot of $ln(NO_3$-N) vs. $\delta^{15}N_{NO3}$, which will be the same as on a plot of $ln(f_d)$ vs. $\delta^{15}N_{NO3}$. In-situ variations in temperature and reaction rates may affect the enrichment factor (Kendall and Aravena, 2000) and this was accounted for by allowing for variation in ε_{15N} within the Monte Carlo analysis. The enrichment factor for $\delta^{18}O_{NO3}$ (ε_{18O}) was calculated by multiplying the $\delta^{15}N_{NO3}$ by a linear coefficient of proportionality determined for each CFO from the slope of the denitrification trend on an isotope cross-plot (see Section 3.2). This approach neglects the effect of mixing of groundwater with differing isotopic values, and is valid if the concentration of NO_3^- in the source is much greater than background concentrations such that the isotopic composition of NO_3^- is dominated by the agriculturally derived end-member.

2.4.2 Quantification of mixing and initial concentrations of Cl^- and NO_3-N

A binary mixing model that also accounts for decreasing NO_3-N concentrations in response to denitrification was used to quantify NO_3^- attenuation by mixing and estimate the initial concentrations of Cl^- and NO_3-N. The measured concentration of Cl^- was assumed to be a function of two end-member mixing, described by

$$Cl = f_m Cl_i + (1 - f_m)Cl_b, \tag{3}$$

where Cl is the measured concentration of Cl^- in the groundwater sample, Cl_i is the concentration of Cl^- at the initial point of entry of the agriculturally derived NO_3^- to the groundwater system, Cl_b is the concentration of Cl^- in the background ambient groundwater, and f_m is the fraction of water in the sample from the source of agriculturally derived Cl^- (and NO_3^-) remaining in the mixture.

The concentration of NO_3-N was also assumed to be a function of two end-member mixing but with an additional coefficient, f_d (the fraction of NO_3-N remaining after denitrification), applied to account for denitrification. The measured NO_3-N concentration was thus described by

$$NO_3\text{-}N = f_d(f_m NO_3\text{-}N_i + (1 - f_m)NO_3\text{-}N_b), \tag{4}$$

where $NO_3\text{-}N$ is the concentration of NO_3-N measured in the groundwater sample, $NO_3\text{-}N_i$ is the concentration of NO_3-N in the source of agriculturally derived NO_3^- at the initial point of entry to the groundwater system, and $NO_3\text{-}N_b$ is the concentration of NO_3-N in the background ambient groundwater. This mixing calculation was only conducted on samples for which NO_3^- dominated total-N (NH_3-N <10% of NO_3-N) so that nitrification of NH_3 could be neglected.

If Cl_i is much greater than Cl_b and $NO_3\text{-}N_i$ is much greater than $NO_3\text{-}N_b$, then f_m is insensitive to background concentrations and these terms can be neglected (see Section 4 for further discussion of this assumption). In this case, Eqs. (3) and (4) reduce to

$$Cl = f_m Cl_i , \tag{5}$$

$$NO_3\text{-}N = f_d(f_m NO_3\text{-}N_i) . \tag{6}$$

Solving Eq. (6) for f_m and substituting into Eq. (5) yields

$$\frac{NO_3\text{-}N_i}{Cl_i} = \frac{1}{f_d}\frac{NO_3\text{-}N}{Cl} . \tag{7}$$

Thus, for each groundwater sample, the ratio of NO_3-N/Cl^- at the initial point of entry of the agriculturally derived NO_3^- to the groundwater system $\left(\frac{NO_3\text{-}N_i}{Cl_i}\right)$ can be simply calculated using measured concentrations, and f_d estimated from NO_3^- isotope data. This provides a relatively simple method to identify agriculturally derived NO_3^- from different sources (e.g., EMS vs. manure piles) if they have different NO_3-N/Cl^- ratios. Estimated Cl_i and $NO_3\text{-}N_i$ are reported as the mid-range value with uncertainty described by the minimum and maximum values. These initial concentrations are at the water table for top-down inputs, or at the saturated point of contact between the EMS and the aquifer for leakage from the EMS. This analysis assumes that a sampled water parcel consists of water with agriculturally derived NO_3^- that entered the aquifer from one source at one point in time and space and has since mixed with natural ambient groundwater. Any NO_3^- produced during nitrification after the anthropogenic source water enters the aquifer is implicitly included in $NO_3\text{-}N_i$. The error in $\frac{NO_3\text{-}N_i}{Cl_i^-}$ was assumed to be dominated by error in the estimated f_d, with the measurement error in NO_3-N and Cl^- considered negligible.

The initial concentrations of the agriculturally derived NO_3^- source ($NO_3\text{-}N_i$ and Cl_i) were estimated by simultaneously solving Eqs. (5) and (6) using Excel Solver (GRG nonlinear). The absolute minimum values of $NO_3\text{-}N_i$ and Cl_i were defined by measured concentrations (e.g., if Cl_i=Cl, f_m=1). Maximum values of $NO_3\text{-}N_i$ and Cl_i were defined based on measured concentrations of NO_3-N and Cl^- in groundwater and manure filtrate (NO_3-N ≤ 150 mg L^{-1} and $Cl^- \leq 1300$ mg L^{-1}; see Section 3.2). These maximum values of $NO_3\text{-}N_i$ and Cl_i correspond to the minimum f_m. The value of f_d was assumed to be the mean f_d estimated from NO_3^- isotopes using Eq. (2), and $\frac{NO_3\text{-}N_i}{Cl_i}$ was required to be within one standard deviation of the estimate from Eq. (7).

The resulting estimates of f_m are reported as the mid-range, with uncertainty described by the minimum and maximum values. Larger values of f_m indicate less mixing (a shorter path for advection-dispersion) and suggest a source close to the well. Smaller values of f_m indicate extensive mixing (a longer path for advection-dispersion) and suggest a source further away from the well. The relative contributions of mixing and denitrification to NO_3^- attenuation at each site were evaluated by comparing f_m and f_d for each sample. This analysis was conducted using isotope values from the samples collected on 1 May 2013 at CFO1, which were combined with the Cl^- and NO_3-N data from 6 June 2013. At CFO4, results from stable isotopes collected on 27 October 2014 were combined with Cl^- and NO_3-N data collected on 7 October 2014.

3. Results

3.1 Site hydrogeology

3.1.1 CFO1

The geology at CFO1 consists of clay and clay-till interspersed with sand layers of varying thickness to the maximum depth of investigation (20 m BG, bedrock not encountered). Hydraulic conductivities (K) calculated from slug tests on wells ranged from 1.2×10^{-7} to 4.2×10^{-5} m-s^{-1} (n=10) for sand, 1.1×10^{-8} to 2.8×10^{-8} m s^{-1} (n=2) for clay-till, and 1.6×10^{-9} to 3.0×10^{-7} m s^{-1} (n=8) for clay. Depth to the water table throughout the study site ranged from 0.5 m at DMW14 to 3.8 m at DMW11. Seasonal water table variations were about 0.5 m with no obvious change in the annual average during the 6-year measurement period. Water table elevation was highest at DMW10 and DMW1 on the west side of the site and lowest at DMW11 on the northeast side of the site (see Supplementary Material). Measured heads indicate groundwater flow from the vicinity of the EMS to the northeast and southeast. Mean horizontal hydraulic gradients at the water table ranged from 4.4×10^{-3} to 1.4×10^{-2} m m^{-1}. Vertical gradients were predominantly downward in the upper 20 m of the profile (mean gradients ranging from 1.8×10^{-3} to 0.18 m m^{-1}), with the exception of DMW11 where the vertical gradient was upward (mean gradient -2.8×10^{-2} m m^{-1}). Using the geometric mean K for the sand (5.0×10^{-6} m s^{-1}) and a lateral head gradient of 1.4×10^{-2} m m^{-1} yields a specific discharge (Darcy flux, q) of 2.2 m y^{-1}. Assuming an effective porosity of 0.3 (Rodvang et al., 1998), the average linear velocity ($\bar{v}$) is 7.4 m y^{-1}. This suggests that, in the absence of attenuation by mixing or denitrification, agriculturally derived NO$_3^-$ could have been transported through the groundwater system by advection about 400 m from the EMS since 1960 and 630 m since 1930.

3.1.2 CFO4

The geology at CFO4 consists of about 5 m of clay (with minor till) underlain by sandstone, to the maximum depth investigated (20 m BG). Hydraulic conductivities measured using slug tests on wells were 1.0×10^{-8} to 1.0×10^{-5} m s^{-1} (n=12) for the clay and sandstone (many shallow wells were screened across the clay-till and into the sandstone) and 1.0×10^{-5} to 2.9×10^{-5} m s^{-1} (n=4) for the sandstone. The depth to water table ranged from 1.0 to 3.4 m, increasing from west to east across the study site. Seasonal water table variations were on the order of 1.5 m with water table declines on the order of 0.3 m y^{-1}. The horizontal hydraulic gradient was consistently from west to east, with a mean gradient at the water table of 3.9×10^{-3} m m^{-1} between BC2 and BMW2 and 4.3×10^{-3} m m^{-1} between BMW2 and BMW7. Vertical hydraulic gradients were 4.2×10^{-2} to 4.6×10^{-2} m m^{-1} downward. Using the geometric mean K for the site (2.9×10^{-5} m s^{-1}) and a lateral head gradient of 4.3×10^{-3} m m^{-1} yields a q of 0.4 m y^{-1}. Assuming an effective porosity of 0.3 yields a $\bar{v}$ of 1.3 m y^{-1}. These values suggest that, in the absence of attenuation by mixing or denitrification, anthropogenic NO$_3^-$ could have been transported through the groundwater systems about 10 m by advection between 1995 and the time of sampling.

3.2 Values and evolution of stable isotopes of nitrate

Manure filtrate from the EMS at CFO1 had δ^{15}N$_{NO3}$ ranging from 0.4 to 5.0‰ and δ^{18}O$_{NO3}$ ranging from 7.1 to 19.0‰. A curve showing the co-evolution of δ^{18}O$_{NO3}$ (mixing of atmospheric δ^{18}O with groundwater-derived δ^{18}O) and δ^{15}N$_{NO3}$ (Rayleigh distillation, $\beta = 1.005$) during nitrification is shown in Fig. 2. Isotopic values in

DMW3, where direct leakage from the EMS was evident, are consistent with partial nitrification following this trend of isotopic evolution ($\delta^{18}O_{NO3}$ of -1.2‰ and $\delta^{15}N_{NO3}$ of 7.8‰).

The range of isotopic values of NO_3^- in groundwater is similar at both sites (Fig. 2). At CFO1, $\delta^{18}O_{NO3}$ ranged from -5.9 to 20.1‰ and $\delta^{15}N_{NO3}$ from -5.2 to 61.0‰. At CFO4, $\delta^{18}O_{NO3}$ ranged from -1.9 to 31.6‰ and $\delta^{15}N_{NO3}$ from -1.3 to 70.5‰. The isotopic values of $\delta^{18}O_{NO3}$ in groundwater are commonly assumed to be derived from a mix of a 1/3 atmospheric-derived oxygen (+23.5‰) and 2/3 water-derived oxygen (Xue et al., 2009). Given the average $\delta^{18}O_{H2O}$ for both sites (-16‰, see Supplementary Material), a 1/3 atmospheric 2/3 groundwater mix would result in a $\delta^{18}O_{NO3}$ of -3.7‰.

At both sites, co-enrichment of $\delta^{18}O_{NO3}$ and $\delta^{15}N_{NO3}$ characteristic of denitrification was evident in some samples (slopes of 0.42 and 0.72 in Fig. 2a). At CFO1, this includes samples from DP10-2, DMW5, DMW11, DMW12, DP11-12b, and DMW13 (and associated core) and some pore water from cores DC15-22 and DC15-23. These samples had NO_3-N concentrations of 0.6 to 23.7 mg L^{-1}, $\delta^{18}O_{NO3}$ ranging from 4.8 to 20.6‰, and $\delta^{15}N_{NO3}$ ranging from 22.9 to 61.3‰. At CFO4, samples exhibiting evidence of denitrification were from BMW2, BMW5, BMW6, BMW7, and BC4. These samples had NO_3-N concentrations ranging from 0.4 to 35.1 mg L^{-1}, $\delta^{18}O_{NO3}$ ranging from 1.6 to 22.1‰, and $\delta^{15}N_{NO3}$ ranging from 20.9 to 70.1‰. Although the isotopic values of DMW5 suggest enrichment by denitrification, the data plot away from the rest of the CFO1 data and close to the denitrification trend at CFO4 (Fig. 2), suggesting these samples were affected by some other process (possibly mixing or nitrification); therefore, the fraction of NO_3-N remaining in this well was not calculated. Also, well DMW3, which clearly receives leakage from the EMS, did not contain substantial NO_3-N and so f_d was not calculated.

The potential range of original isotopic values of the NO_3^- source prior to denitrification (R_0) varied from 5 to 27‰ for $\delta^{15}N_{NO3}$ and from -2 to 7‰ for $\delta^{18}O_{NO3}$ based on isotopic values measured during this study (Fig. 2a). These values are consistent with literature values for manure-sourced NO_3^-, which report $\delta^{15}N_{NO3}$ ranging from 5 to 25‰ and $\delta^{18}O_{NO3}$ ranging from -5 to 5‰ (Wassenaar, 1995; Wassenaar et al., 2006; Singleton et al., 2007; McCallum et al., 2008; Baily et al., 2011).

The enrichment factor of $\delta^{15}N_{NO3}$ was defined by a normal distribution with a mean of -10‰ and standard deviation of 2.5‰. At CFO1, the coefficient of proportionality between the enrichment factor of $\delta^{15}N_{NO3}$ and $\delta^{18}O_{NO3}$ was described by a normal distribution with mean of 0.72 and standard deviation of 0.05. At CFO4, the coefficient of proportionality was also described by a normal distribution with a mean of 0.42 and standard deviation of 0.035 (see Fig. 2a). These enrichment factors are consistent with values from denitrification studies that report ε_{15N} ranging from -4.0 to -30.0‰ and ε_{18O} ranging from -1.9 to -8.9‰ (Vogel et al., 1981; Mariotti et al., 1988; Böttcher et al., 1990; Spalding and Parrott, 1994; Mengis et al., 1999; Pauwels et al., 2000; Otero et al., 2009).

3.3 Distribution and sources of agricultural nitrate in groundwater

At both sites TN concentrations in filtrate from the EMS and catch-basin were generally an order of magnitude larger than concentrations in groundwater (Table 2). The one exception is well DMW3 at CFO1 which intercepted direct leakage from the EMS (see 3.3.1 for further discussion of this well), In the EMS filtrate, N was predominately organic-N (TON up to 71%) or NH_3-N (up to 90%), with NO_x-N <0.1% of TN. In the catch-basin TON was >99% of TN. In groundwater TN concentrations ranged from <0.25 to 84.6 mg L^{-1}, and this N was predominantly NO_3^- (again, with the exception of DMW3).

3.3.1 CFO1

Agriculturally derived NO_3^- was predominantly restricted to the upper 20 m (or less) at CFO1 (NO_3-N $\leq$ 0.2 mg L^{-1} and Cl$^-$ $\leq$ 57 mg L^{-1} in seven wells screened at 20 m). The one exception was DP11-12b, which had up to 4.1 mg L^{-1} of NO_3-N. The southeast portion of the site also does not appear to have been significantly contaminated by agriculturally derived NO_3^-, with NO_3-N concentrations < 1 mg L^{-1} in five water table wells (DMW4, DMW6, DMW14, DMW15, DMW16). In DMW6, Cl$^-$ and TN concentrations were elevated (see Supplementary Material) but NO_3-N concentrations were < 2 mg L^{-1}. Collectively, these data suggest the catch basin is not a significant source of NO_3^- to the groundwater at this site.

Leakage of manure slurry from the EMS at CFO1 is clearly indicated by the data from DMW3, which feature the highest concentrations of TN in groundwater (up to 548 mg L^{-1}) and elevated Cl$^-$, HCO$_3^-$, and DOC in concentrations similar to EMS manure filtrate (see Supplementary Material). Nevertheless, NO_3-N concentrations in this well were consistently low (1.1 $\pm$ 2.7 mg L^{-1}, n=22). The potential for nitrification in the vicinity of this well is indicated by NO_2-N production (2.7 $\pm$ 8.3 mg L^{-1}, n=22). However, the data demonstrate that only a small proportion of the NH_3-N in DMW3 (373.4 $\pm$ 79.4 mg L^{-1}, n=22) could have been converted to NO_3^- within the subsurface (NO_3-N in groundwater $\leq$ 66 mg L^{-1}) (NO_3-N/Cl$^-$ ratio of 0.95).

The maximum NO_3-N concentration in groundwater was measured in core sample DC15-23 (clay at 2 m bgl, 7 m hydraulically downgradient of DMW3). The NO_3-N in this core sample was most likely introduced into the groundwater system by vertical infiltration or diffusion from above. Pore water extracted from the unsaturated zone (sand) at the top of this core profile contained 865 mg L^{-1} of NO_3-N and had a NO_3-N/Cl$^-$ ratio of 1.04, consistent with the ratio of 0.95 in the core sample.

Contamination by agricultural NO_3^- that exceeds the drinking water guidelines (NO_3-N > 10 mg L^{-1}) was observed in wells up to 40 m hydraulically downgradient of the EMS (DMW13, DP10-2) and in well DMW11 situated 470 from the EMS (Fig. 3). DMW1, located upgradient of the EMS, also had concentrations of NO_3-N > 10 mg L^{-1} with an increasing trend, but the source of this NO_3^- is not clear. DMW2 and DMW12 also had NO_3-N concentrations that were elevated but did not exceed the drinking water guideline ($\leq$ 3.7 mg L^{-1}).

Given the evidence of incomplete partial nitrification in DMW3, the NO_3-N/Cl$^-$ ratio of contamination from the EMS was assumed to be best represented by DP10-2, which is located directly downgradient of the EMS. Data for this well indicate values of NO_3-N/Cl$^-$ predominantly ranging from 0.1 to 0.3 with NO_3-N_i/Cl_i estimated at 0.3 $\pm$ 0.13 (Fig. 4). Advective transport from DMW3 is also the likely source of NO_3-N (up to 21.1 mg L^{-1}) within the sand between 6 and 12 m depth in DC15-23. NO_3-N/Cl$^-$ ratios in these samples ranged from 0.07 to 0.31, consistent with DP10-2. Stable isotope values in pore water from this sand layer do not indicate substantial denitrification ($\delta^{18}O \leq$ 5.9‰, $\delta^{15}N \leq$ 16.7‰), suggesting these ratios will be similar to the initial ratios at the point of entry to the groundwater system.

In contrast, the ratio of NO_3-N_i/Cl_i in DMW13 (33 m downgradient from DP10-2) was 0.75 $\pm$ 0.29 is more similar to the NO_3-N/Cl$^-$ ratio in DC15-23 at 2 m (0.95), which is interpreted as reflecting a top-down source. The NO_3^- in DMW13 is therefore unlikely to be sourced solely from leakage from the EMS, and could be sourced from the adjacent dairy pens or a temporary manure pile that was observed adjacent to this well during core collection in 2015 (or a combination of EMS and top-down sources).

The NO_3-N_i/Cl_i ratio in DMW12 is not inconsistent with an EMS source, but the hydraulic gradient between DMW2 and DMW12 is negligible, indicating a lack of driving force for advective transport from the EMS towards

DMW12. This is also the case for well DMW1, which is upgradient of the EMS but had elevated NO_3-N concentrations (6.5 ± 3.6, n=18). The source of nitrate in these wells is therefore unlikely to be related to leakage from the EMS, but alternative sources (i.e., nearby temporary manure piles) are not known.

Well DMW11 had consistently low NO_3-N/Cl^- ratios (< 0.05). The $NO_3\text{-}N_i/Cl_i$ ratio indicated by DMW11 was similar to DP10-2, but estimates of Cl_i indicate Cl^- sourced from inputs with three-fold higher Cl^- concentrations than the source to DP10-2 (Fig. 4b). Well DMW11 is located hydraulically downgradient of feedlot pens and adjacent to a solid manure storage area. Well DMW11 is also in a local topographic low and is likely receiving NO_3-N and Cl^- from surface runoff and infiltration in addition to subsurface groundwater flow. Well DMW11 had high $NO_3\text{-}N_i$ and Cl_i consistent with measured values in that well, indicating a local top-down source that is likely the nearby solid manure pile.

3.3.2 CFO4

At CFO4, measured data indicate that effects from agricultural operations on NO_3^- concentrations in groundwater are restricted to the upper 15 m of the subsurface. NO_3-N concentrations in wells screened at 15 m depth were < 0.5 mg L^{-1}, with the exception of one sample from BP10-15w (May 2012) with 4.3 mg L^{-1} of NO_3-N. Water table wells in the west and north of the study site (BC1, BC2, and BC3) also indicate negligible impacts of agricultural operations, with Cl^- < 10 mg L^{-1} and NO_3-N < 0.1 mg L^{-1}.

Concentrations of NO_3-N > 10 mg L^{-1} were measured in three water table wells (BMW2, BMW3, BMW4) installed adjacent to the EMS (Fig. 5). Of these, BMW2 had much higher Cl^- concentrations (502 ± 97 mg L^{-1}, n=22), and therefore lower NO_3-N/Cl^- ratios (< 0.05). Given the elevated Cl^- concentrations in this well were consistent with concentrations in the EMS, direct leakage from the EMS was assumed to be the source. Stable isotopes of NO_3^- indicate substantial denitrification in BMW2, with estimated $NO_3\text{-}N_i \geq 127$ mg L^{-1} and an $NO_3\text{-}N_i/Cl_i$ ratio of 0.1 to 0.3 (Fig. 6). This ratio is consistent with data from well BMW4, which is immediately adjacent to the EMS (on the upgradient side) and likely reflects leakage from the EMS without denitrification (based on stable isotopes of NO_3^-). NO_3-N/Cl^- ratios measured in BMW4 were predominantly 0.1 to 0.3, consistent with the reconstructed $NO_3\text{-}N_i/Cl_i$ ratio in BMW2.

Agriculturally derived NO_3^- in other wells not immediately adjacent to the EMS is unlikely to be related to leakage from the EMS. Wells BMW5 and BMW7 are 60 and 140 m hydraulically downgradient from the EMS, respectively. $NO_3\text{-}N_i/Cl_i$ ratios in these wells were not inconsistent with BMW2 (i.e., the range of values overlap), but advective transport is only likely to have transported solutes around 10 m since the EMS was installed (see Section 3.1.2). As such, the source of NO_3-N in these wells is likely the dairy pens rather than the EMS. Concentrations of NO_3-N > 10 mg L^{-1} were also measured in BC4, which is located 95 m hydraulically upgradient of the EMS. The ratio of $NO_3\text{-}N_i/Cl_i$ at BC4 was the highest at CFO4 (0.6) and did not overlap with BMW2. This indicates that the NO_3^- in this well was sourced from an adjacent manure pile, which was observed during the study.

3.4 Mechanisms of attenuation of agriculturally derived NO_3^-

Attenuation of agriculturally derived NO_3^- in groundwater is dominated by denitrification at CFO1 and CFO4, with estimates of f_m consistently higher than estimates of f_d (Table 3, Fig. 7, Table S10). Calculated f_d values suggest that at least half of the NO_3-N present at the initial point of entry to the groundwater system has been

removed by denitrification. Comparison of NO_3-N_{mix} (the concentration of NO_3-N that would be measured if mixing was the only attenuation mechanism) with measured concentrations (which reflect attenuation by both mixing and denitrification) suggests that the sample from 20 m depth (DP11-12b) is the only sample that would be below the drinking water guideline if mixing was the only attenuation mechanism (Fig. 8).

5   At both sites, the stable isotope values of NO_3^- indicate that denitrification proceeds within metres of the source. At CFO1, calculated f_d in well DP10-2 (2 m from the EMS) is 0.52 ± 0.22; at CFO4, f_d in well BMW2 (3 m from the EMS) is 0.13 ± 0.06. Denitrification also substantially attenuated NO_3-N concentrations in wells where the source is not the EMS but instead is adjacent solid manure piles (e.g., DMW11 at CFO1, BC4 at CFO4). In BMW6 at CFO4, denitrification completely attenuated the agriculturally derived NO_3^-. This well had negligible NO_3-N

10    $(0.4 \pm 0.2$ mg L^{-1}, n=8) and the lowest f_d of 0.01. Measured DOC in this well was consistent with other wells at both sites (6.9 ± 1.7 mg L^{-1}, n=3), suggesting DOC depletion does not limit denitrification at these CFO operations. Calculated f_d and f_m should decrease with increasing subsurface residence time and distance from source. Data from wells support the source identification based on concentrations of NO_3-N and Cl^- and NO_3-N/Cl^- ratios (see Section 3.3). Well DMW11 (470 m from the EMS) had the highest f_m at CFO1 (0.83), indicating less mixing and

15   suggesting the anthropogenic source of NO_3^- in this well is relatively close, which is consistent with the adjacent the solid manure pile being the source of NO_3^- to this well. At CFO4, well BMW2, which is adjacent to the EMS, had the highest f_m (0.92), indicating the least attenuation of NO_3 by mixing and consistent with the EMS being the source of NO_3^- to this well.

20   **4. Discussion**

Agriculturally derived NO_3^- at these two sites with varying lithology is generally restricted to depths < 20 m, consistent with previous studies at CFOs (Robertson et al., 1996; Rodvang and Simpkins, 2001; Rodvang et al., 2004; Kohn et al., 2016). Attenuation of agriculturally derived NO_3^- in groundwater is a spatially varying combination of mixing and denitrification, with denitrification playing a greater role than mixing at both sites. In

25   the samples for which f_d could be determined, denitrification reduced NO_3^- concentrations by at least half and, in some cases, back to background concentrations. Given that the range of source isotopic composition was allowed to vary to its maximum justifiable extent, these quantitative estimates of denitrification based on stable isotopes of NO_3^- are likely to be conservative. Denitrification appears to proceed within metres of the NO_3^- source, suggesting relatively short residence times and redox conditions at the water table may be conducive to

30   denitrification reactions (Critchley et al., 2014; Clague et al., 2015).

The substantial role of denitrification within the saturated glacial sediments at these study sites indicates the potential for significant attenuation of agriculturally derived NO_3^- by denitrification in similar groundwater systems across the North American interior and Europe (Ernstsen et al., 2015; Zirkle et al., 2016). Denitrification in the unsaturated zone is limited by low water contents and oxic conditions, resulting in substantial stores of NO_3^-

35   in vadose zones (Turkeltaub et al., 2016; Ascott et al., 2017). NO_3^- in water that is removed rapidly from site is also unlikely to be substantially attenuated by denitrification due to oxic conditions and rapid transit times (Ernstsen et al., 2015). Therefore, water management focussed on reducing the effects of NO_3^- contamination in similar hydrogeological settings to this study should aim to maximize infiltration into the saturated zone where

NO$_3^-$ concentrations can be naturally attenuated, provided that local groundwater isn't used for potable water supply.

Infiltration of NO$_3^-$ rich water that has passed through temporary solid manure piles and dairy pens has resulted in groundwater NO$_3$-N concentrations as high as those associated with leakage from the EMS (e.g., DMW11, DMW13, BC4). At CFO4, this is in spite of the presence of clay at surface, which is attributable to secondary porosity in the upper part of the profile that has led to hydraulic conductivities comparable to sand. This is consistent with the findings of Showers et al. (2008), who investigated sources of NO$_3^-$ at an urbanized dairy farm in North Carolina, USA. Construction of EMS facilities in Alberta has been regulated under the Agriculture Operation Practices Act since 2002, which requires them to be lined with clay to minimise leakage (Lorenz et al., 2014). The results of this study suggest that on-farm waste management should increasingly focus on minimising temporary manure piles that are in direct contact with the soil to reduce NO$_3^-$ contamination associated with dairy farms and feedlots.

The absence of direct leakage from the EMS at CFO4 suggests that saturation within the clay lining of the EMS has limited the development of extensive secondary porosity that would allow rapid water percolation (Baram et al., 2012). Elevated NH$_3$-N concentrations in the water table well at the southeast corner of the EMS at CFO1 (DMW3) do indicate direct leakage from the EMS, but because nitrification within the EMS is minimal, this has not resulted in elevated NO$_3$-N in this well. Two possibilities for the fate of NH$_3$-N in DMW3 are attenuation by cation exchange and oxidation to NO$_3$-N within the groundwater system. Measured NO$_3$-N concentrations in groundwater represent only a small fraction ($\leq 10\%$) of NH$_3$-N within the EMS (or DMW3), suggesting oxidation to NO$_3^-$ within the aquifer may be limited. Further work is required to assess the importance of cation exchange as an attenuation mechanism for direct leakage from the EMS at this site.

The sources of manure-derived NO$_3^-$ (manure piles vs. EMS) are distinguishable based on $NO_3\text{-}N_i/Cl_i$ ratios, provided there is also an understanding of the history of each site, local hydrogeology, and potential sources. Estimation of $NO_3\text{-}N_i/Cl_i$ assumes that background concentrations could be neglected in the mixing calculation. The error associated with this assumption increases as source concentrations and measured concentrations approach background concentrations. At these study sites, background concentrations are likely to be < 20 mg L^{-1} for Cl$^-$ and < 1 mg L^{-1} for NO$_3$-N. Based on these values, estimated $NO_3\text{-}N_i$ values are at least 20 times background NO$_3$-N concentrations, and over 100 times background concentrations in some wells. The estimated Cl_i values are at least three times background concentrations at CFO1 and at least 10 times background concentrations at CFO4. In this study we applied a two-end member mixing model and assumed that background concentrations can be neglected. The error introduced by neglecting background concentrations was assessed by comparing f_m calculated with and without background concentrations included, using the full range of values in this study (Fig. 9). Neglecting background concentrations results in overestimation of f_m (i.e. underestimation of the amount of attenuation mixing) with the largest errors when measured concentrations are close to background concentrations. For Cl$^-$ the maximum difference of 0.13 is in the mid-range of f_m values. For NO$_3$-N, the difference is consistently < 0.1 with the largest errors at the lowest values of f_m. The uncertainty in f_m is primarily related to uncertainty in the initial concentrations (Cl_i and $NO_3\text{-}N_i$), which depends on measured Cl$^-$ and NO$_3$-N. The largest uncertainties in $NO_3\text{-}N_i$ and Cl_i correspond to the lowest measured concentrations (i.e., furthest from the upper limit), with less uncertainty at higher measured concentrations as they approach the maximum values. Temporal variability in

NO_3-N_i/Cl_i for each source could not be determined based on the snapshot isotope sampling conducted, but this could be investigated by measuring NO_3^- isotopes in conjunction with NO_3-N and Cl^- at multiple times.

Although applicable at these sites, this approach may not be valid at other sites if additional sources of NO_3 in groundwater (e.g. fertilizer or nitrification) are significant, or if NO_3 concentrations in groundwater are naturally elevated (Hendry et al., 1984). The combination of the approach outlined here with measurement of groundwater age indicators would allow for better constraints on groundwater flow velocities and determination of denitrification rates (Böhlke and Denver, 1995; Katz et al., 2004; McMahon et al., 2004; Clague et al., 2015).

Nitrate isotope values in groundwater at the two CFOs studied are generally consistent with previous studies reporting denitrification of manure-derived NO_3^- at dairy farms (Wassenaar, 1995; Wassenaar et al., 2006; Singleton et al., 2007; McCallum et al., 2008; Baily et al., 2011). However, a number of groundwater samples collected for the present study had relatively enriched $\delta^{18}O_{NO3}$ (> 15 ‰) with depleted $\delta^{15}N_{NO3}$ (< 15‰). Some of these isotopic values are within the range previously reported for NO_3^- derived from inorganic fertilizer ($\delta^{15}N_{NO3}$ from -3 to 3‰ and $\delta^{18}O_{NO3}$ from -5 to 25‰), with the $\delta^{18}O_{NO3}$ depending on whether the NO_3^- is from NH_4^+ or NO_3^- in the fertilizer (Mengis et al., 2001; Wassenaar et al., 2006; Xue et al., 2009). To the best of our knowledge, however, no inorganic fertilizers have been applied at these study sites. Another potential source is NO_3^- derived from soil organic N, but this should have $\delta^{15}N_{NO3}$ values of 0 to 10‰ and $\delta^{18}O_{NO3}$ values of -10 to 15‰ (Durka et al., 1994; Mayer et al., 2001; Mengis et al., 2001; Xue et al., 2009; Baily et al., 2011). Incomplete nitrification of NH_4^+ can result in $\delta^{15}N_{NO3}$ lower than the manure source (Choi et al., 2003), but as there was no measurable NH_3-N in these samples this is also unlikely. These isotope values may reflect the influence of NO_3^- from precipitation, which usually has values ranging from -5 to 5‰ for $\delta^{15}N_{NO3}$ and 40 to 60‰ for $\delta^{18}O_{NO3}$, and has been reported to dominate NO_3^- isotope values of groundwater under forested landscapes (Durka et al., 1994). Alternatively, they may be affected by microbial immobilization and subsequent mineralization and nitrification, which can mask the source $\delta^{18}O_{NO3}$ in aquifers with long residence times (Mengis et al., 2001; Rivett et al., 2008). The isotopic values of NO_3^- in the manure filtrate from the EMS at CFO1, were generally inconsistent with values for manure-sourced NO_3^- reported in other groundwater studies (Wassenaar, 1995; Wassenaar et al., 2006; Singleton et al., 2007; McCallum et al., 2008a; Baily et al., 2011). This is likely to be because nitrification within the EMS was negligible (NO_3-N <0.7 mg L^{-1}), such that the isotopic values of NO_3-N in the manure filtrate reflect volatilization of NH_3 and partial nitrification within the EMS. $\delta^{18}O_{NO3}$ values may also have been affected by evaporative enrichment of the $\delta^{18}O_{H2O}$ being incorporated into NO_3^- (Showers et al., 2008).

5. Conclusions

A mixing model constrained by quantitative estimates of denitrification from isotopes substantially improved our understanding of nitrate contamination at these sites. This novel approach has the potential to be widely applied as a tool for monitoring and assessment of groundwater in complex agricultural settings. Even though these sites are dominated by clay-rich glacial sediments, the input of NO_3^- to groundwater from temporary manure piles and pens resulted in comparable (or greater) NO_3-N concentrations than leakage from the EMS. On-farm management of manure waste should increasingly focus on limiting manure piles that are in direct contact with the soil to limit NO_3^- contamination of groundwater. Nitrate attenuation at both sites is dominated by denitrification, which is evident even in wells directly adjacent to the NO_3^- source. On-site denitrification reduced agriculturally derived NO_3^- concentrations by at least half and, in some wells, completely. These results indicate that infiltration to

groundwater systems in glacial sediments where NO_3^- can be naturally attenuated is likely to be preferable to off-farm export via runoff or drainage networks, provided that local groundwater isn't a potable water source.

Acknowledgements

This research was supported by Alberta Agriculture and Forestry (AAF) and the Natural Resources Conservation Board (NRCB), who provided assistance with field work and laboratory analysis. Funding was also provided by a Natural Sciences and Engineering Research Council of Canada (NSERC) Industrial Research Chair (IRC) (184573) awarded to MJH. The authors thank Barry Olson at AAF for reviewing the manuscript. Our thanks also to the local producers, whose cooperation made this research possible.

References

Arauzo, M.: Vulnerability of groundwater resources to nitrate pollution: A simple and effective procedure for delimiting Nitrate Vulnerable Zones, Sci. Total Environ., 575, 799-812, 10.1016/j.scitotenv.2016.09.139, 2017.

Aravena, R., Evans, M., and Cherry, J. A.: Stable isotopes of oxygen and nitrogen in source identification of nitrate from septic systems, Groundwater, 31, 180-186, 1993.

Ascott, M. J., Gooddy, D. C., Wang, L., Stuart, M. E., Lewis, M. A., Ward, R. S., and Binley, A. M.: Global patterns of nitrate storage in the vadose zone, Nat. Commun., 8, 1416, 10.1038/s41467-017-01321-w, 2017.

Baily, A., Rock, L., Watson, C., and Fenton, O.: Spatial and temporal variations in groundwater nitrate at an intensive dairy farm in south-east Ireland: Insights from stable isotope data, Agric. Ecosyst. Environ., 144, 308-318, 2011.

Baram, S., Kurtzman, D., and Dahan, O.: Water percolation through a clayey vadose zone, J. Hydrol., 424-425, 165-171, https://doi.org/10.1016/j.jhydrol.2011.12.040, 2012.

Böhlke, J. K., and Denver, J. M.: Combined use of groundwater dating, chemical, and isotopic analyses to resolve the history and fate of nitrate contamination in two agricultural watersheds, Atlantic Coastal Plain, Maryland, Water Resour. Res., 31, 2319-2339, 10.1029/95WR01584, 1995.

Böttcher, J., Strebel, O., Voerkelius, S., and Schmidt, H. L.: Using isotope fractionation of nitrate-nitrogen and nitrate-oxygen for evaluation of microbial denitrification in a sandy aquifer, J. Hydrol., 114, 413-424, 10.1016/0022-1694(90)90068-9, 1990.

Bourke, S. A., Cook, P. G., Dogramaci, S., and Kipfer, R.: Partitioning sources of recharge in environments with groundwater recirculation using carbon-14 and CFC-12, J. Hydrol., 525, 418-428, 2015a.

Bourke, S. A., Turchenek, J., Schmeling, E. E., Mahmood, F. N., Olson, B. M., and Hendry, M. J.: Comparison of continuous core profiles and monitoring wells for assessing groundwater contamination by agricultural nitrate, Ground Water Monit. Remediat., 35, 110-117, 2015b.

Choi, W.-J., Lee, S.-M., and Ro, H.-M.: Evaluation of contamination sources of groundwater NO_3^- using nitrogen isotope data: A review, Geosci. J., 7, 81-87, 2003.

Clague, J. C., Stenger, R., and Clough, T. J.: Evaluation of the stable isotope signatures of nitrate to detect denitrification in a shallow groundwater system in New Zealand, Agric. Ecosyst. Environ., 202, 188-197, 10.1016/j.agee.2015.01.011, 2015.

Clark, I. D., and Fritz, P.: Environmental Isotopes in Hydrogeology, CRC Press, 1997.

Critchley, K., Rudolph, D., Devlin, J., and Schillig, P.: Stimulating in situ denitrification in an aerobic, highly permeable municipal drinking water aquifer, J. Contam. Hydrol., 171, 66-80, 2014.

Deutsch, B., Mewes, M., Liskow, I., and Voss, M.: Quantification of diffuse nitrate inputs into a small river system using stable isotopes of oxygen and nitrogen in nitrate, Org. Geochem., 37, 1333-1342, 10.1016/j.orggeochem.2006.04.012, 2006.

Dogramaci, S., Skrzypek, G., Dodson, W., Grierson, P.F.: Stable isotope and hydrochemical evolution of groundwater in the semi-arid Hamersley Basin of subtropical northwest Australia, J. Hydrol., 475, 281-293, 10.1016/j.jhydrol.2012.10.004, 2012.

Durka, W., Schulze, E.-D., Gebauer, G., and Voerkeliust, S.: Effects of forest decline on uptake and leaching of deposited nitrate determined from ^{15}N and ^{18}O measurements, Nature, 372, 765-767, 1994.

Ernstsen, V., Olsen, P., and Rosenbom, A. E.: Long-term monitoring of nitrate transport to drainage from three agricultural clayey till fields, Hydrol. Earth Syst. Sci., 19, 3475-3488, 10.5194/hess-19-3475-2015, 2015.

Fan, A. M., and Steinberg, V. E.: Health implications of nitrate and nitrite in drinking water: An update on methemoglobinemia occurrence and reproductive and developmental toxicity, Regul. Toxicol. Pharmacol., 23, 35-43, 10.1006/rtph.1996.0006, 1996.

Fukada, T., Kisock, K.M., Dennis, P.F., Grischek, T.: A dual isotope approach to identify denitrification in groundwater at a river-bank infiltration site, Water Res., 37, 3070-3078, 2003.

Galloway, J. N., Townsend, A. R., Erisman, J. W., Bekunda, M., Cai, Z., Freney, J. R., Martinelli, L. A., Seitzinger, S. P., and Sutton, M. A.: Transformation of the nitrogen cycle: Recent trends, questions, and potential solutions, Science, 320, 889-892, 10.1126/science.1136674, 2008.

Granger, J., Sigman, D. M., Lehmann, M. F., and Tortell, P. D.: Nitrogen and oxygen isotope fractionation during dissimilatory nitrate reduction by denitrifying bacteria, Limnol. Oceanogr., 53, 2533-2545, 10.4319/lo.2008.53.6.2533, 2008.

Green, C. T., Böhlke, J. K., Bekins, B. A., and Phillips, S. P.: Mixing effects on apparent reaction rates and isotope fractionation during denitrification in a heterogeneous aquifer, Water Resour. Res., 46, 10.1029/2009WR008903, 2010.

Gulis, G., Czompolyova, M., and Cerhan, J. R.: An ecologic study of nitrate in municipal drinking water and cancer incidence in Trnava District, Slovakia, Environ. Res., 88, 182-187, 10.1006/enrs.2002.4331, 2002.

Hautman, D. P., and Munch, D. J.: Method 300.1 Determination of inorganic anions in drinking water by ion chromatography, US Environmental Protection Agency, Cincinnati, OH, 1997.

Hendry, M. J., Barbour, S. L., Novakowski, K., and Wassenaar, L. I.: Paleohydrogeology of the Cretaceous sediments of the Williston Basin using stable isotopes of water, Water Resour. Res., 49, 4580-4592, 2013.

Hendry, M. J., McReady, R.G., Gould, W.D.: Distribution and evolution of nitrate in a glacial till of sourther Alberta, Canada, J. Hydrol., 70, 177-198, 1984.

Ji, X., Runtin, X., Hao, Y., Lu, J., Quantitative identification of nitrate pollution sources and uncertainty analysis based on dual isotope approach in an agricultural watershed, Environ. Pollution, 229, 586-594, 2017.

Joerin, C., Beven, K. J., Iorgulescu, I., and Musy, A.: Uncertainty in hydrograph separations based on geochemical mixing models, J. Hydrol., 255, 90-106, 2002.

Katz, B. G., Chelette, A. R., and Pratt, T. R.: Use of chemical and isotopic tracers to assess nitrate contamination and ground-water age, Woodville Karst Plain, USA, J. Hydrol., 289, 36-61, 10.1016/j.jhydrol.2003.11.001, 2004.

Kaushal, S. S., Groffman, P. M., Band, L. E., Elliott, E. M., Shields, C. A., and Kendall, C.: Tracking nonpoint source nitrogen pollution in human-impacted watersheds, Environ. Sci. Technol., 45, 8225-8232, 10.1021/es200779e, 2011.

Kendall, C., and Aravena, R.: Nitrate isotopes in groundwater systems, in: Environmental Tracers in Subsurface Hydrology, edited by: Cook, P., and Herczeg, A., Springer US, 261-297, 2000.

Kimble, J. M., Bartlett, R. J., McIntosh, J. L., and Varney, K. E.: Fate of nitrate from manure and inorganic nitrogen in a clay soil cropped to continuous corn, J. Environ. Qual., 1 (4), 1972.

Kohn, J., Soto, D. X., Iwanyshyn, M., Olson, B., Kalischuk, A., Lorenz, K., and Hendry, M. J.: Groundwater nitrate and chloride trends in an agriculture-intensive area in southern Alberta, Canada, Water Qual. Res. J., 51, 47-59, 10.2166/wqrjc.2015.132, 2016.

Komor, S. C., and Anderson, H. W.: Nitrogen isotopes as indicators of nitrate sources in Minnesota sand-plain aquifers, Ground Water, 31, 260-270, 1993.

Lentz, R.D., Lehrsch, G.A., Temporal changes in δ^{15}N-and δ^{18}O of nitrate nitrogen and H_2O in shallow groundwater: Transit time and nitrate-source implications for an irrigated tract in southern Idaho, Agric. Water Man., 212, 126-135, 2019.

Liu, C.-Q., Li, S.-L., Lang, Y.-C., and Xiao, H.-Y.: Using $\delta15$N-and $\delta18$O-values to identify nitrate sources in karst ground water, Guiyang, Southwest China, Environ. Sci. Technol., 40, 6928-6933, 2006.

Lorenz, K., Iwanyshyn, M., Olson, B., Kalischuk, A., and Pentland, J. (Eds.): Livestock Manure Impacts on Groundwater Quality in Alberta Project 2008 to 2015: 2008 to 2011 Progress Report. Alberta Agriculture and Rural Development, Lethbridge, Alberta, Canada. 316 pp., 2014.

Mariotti, A., Landreau, A., and Simon, B.: ^{15}N isotope biogeochemistry and natural denitrification process in groundwater: Application to the chalk aquifer of northern France, Geochim. Cosmochim. Acta, 52, 1869-1878, 1988.

Mayer, B., Bollwerk, S. M., Mansfeldt, T., Hütter, B., and Veizer, J.: The oxygen isotope composition of nitrate generated by nitrification in acid forest floors, Geochim. Cosmochim. Acta, 65, 2743-2756, 2001.

McCallum, J. E., Ryan, M. C., Mayer, B., and Rodvang, S. J.: Mixing-induced groundwater denitrification beneath a manured field in southern Alberta, Canada, Appl. Geochem., 23, 2146-2155, 2008.

McMahon, P. B., Böhlke, J. K., and Christenson, S. C.: Geochemistry, radiocarbon ages, and paleorecharge conditions along a transect in the central High Plains aquifer, southwestern Kansas, USA, Appl. Geochem., 19, 1655-1686, 2004.

Menció, A., Mas-Pla, J., Otero, N., Regàs, O., Boy-Roura, M., Puig, R., Bach, J., Domènech, C., Zamorano, M., Brusi, D., and Folch, A.: Nitrate pollution of groundwater; all right…, but nothing else?, Sci. Total Environ., 539, 241-251, 2016.

Mengis, M., Schif, S. L., Harris, M., English, M. C., Aravena, R., Elgood, R. J., and MacLean, A.: Multiple geochemical and isotopic approaches for assessing ground water NO^{3-} elimination in a riparian zone, Ground Water, 37, 448-457, 1999.

Mengis, M., Walther, U., Bernasconi, S. M., and Wehrli, B.: Limitations of using δ^{18}O for the source identification of nitrate in agricultural soils, Environ. Sci. Technol., 35, 1840-1844, 2001.

Otero, N., Torrentó, C., Soler, A., Menció, A., and Mas-Pla, J.: Monitoring groundwater nitrate attenuation in a regional system coupling hydrogeology with multi-isotopic methods: The case of Plana de Vic (Osona, Spain), Agric. Ecosyst. Environ., 133, 103-113, 2009.

Pastén-Zapata, E., Ledesma-Ruiz, R., Harter, T., Ramírez, A. I., and Mahlknecht, J.: Assessment of sources and fate of nitrate in shallow groundwater of an agricultural area by using a multi-tracer approach, Sci. Total Environ., 470-471, 855-864, 2014.

Pauwels, H., Foucher, J.-C., and Kloppmann, W.: Denitrification and mixing in a schist aquifer: Influence on water chemistry and isotopes, Chem. Geol., 168, 307-324, 2000.

Power, J. F., and Schepers, J. S.: Nitrate contamination of groundwater in North America, Agric., Ecosyst. Environ., 26, 165-187, 1989.

Rivett, M. O., Buss, S. R., Morgan, P., Smith, J. W., and Bemment, C. D.: Nitrate attenuation in groundwater: A review of biogeochemical controlling processes, Water Res., 42, 4215-4232, 2008.

Robertson, W., Russell, B., and Cherry, J.: Attenuation of nitrate in aquitard sediments of southern Ontario, J. Hydrol., 180, 267-281, 1996.

Rodvang, S., and Simpkins, W.: Agricultural contaminants in Quaternary aquitards: A review of occurrence and fate in North America, Hydrogeol. J., 9, 44-59, 2001.

Rodvang, S., Mikalson, D., and Ryan, M.: Changes in ground water quality in an irrigated area of southern Alberta, J. Environ. Qual., 33, 476-487, 2004.

Rodvang, S. , Schmidt-Bellach, R., and Wassenaar, L. : Nitrate in groundwater below irrigated fields, Alberta Agriculture, Food and Rural Development, 1998.

Saffigna, P. G., and Keeney, D. R.: Nitrate and chloride in ground water under irrigated agriculture in central Wisconsin, Ground Water, 15, 170-177, 1977.

Showers, W. J., Genna, B., McDade, T., Bolich, R., and Fountain, J. C.: Nitrate contamination in groundwater on an urbanized dairy farm, Environ. Sci. Technol., 42, 4683-4688, 10.1021/es071551t, 2008.

Sigman, D. M., Casciotti, K. L., Andreani, M., Barford, C., Galanter, M., and Böhlke, J. K.: A bacterial method for the nitrogen isotopic analysis of nitrate in seawater and freshwater, Anal. Chem., 73, 4145-4153, 10.1021/ac010088e, 2001.

Singleton, M., Esser, B., Moran, J., Hudson, G., McNab, W., and Harter, T.: Saturated zone denitrification: Potential for natural attenuation of nitrate contamination in shallow groundwater under dairy operations, Environ. Sci. Technol., 41, 759-765, 2007.

Smith, R. L., Garabedian, S. P., and Brooks, M. H.: Comparison of denitrification activity measurements in groundwater using cores and natural-gradient tracer tests, Environ. Sci. Technol., 30, 3448-3456, 1996.

Spalding, R. F., and Exner, M. E.: Occurrence of nitrate in groundwater—A review, J. Environ. Qual., 22, 392-402, 1993.

Spalding, R. F., and Parrott, J. D.: Shallow groundwater denitrification, Sci. Total Environ., 141, 17-25, 1994.

Tesoriero, A. J., Liebscher, H., and Cox, S. E.: Mechanism and rate of denitrification in an agricultural watershed: Electron and mass balance along groundwater flow paths, Water Resour. Res., 36, 1545-1559, 2000.

Turkeltaub, T., Kurtzman, D., and Dahan, O.: Real-time monitoring of nitrate transport in the deep vadose zone under a crop field – Implications for groundwater protection, Hydrol. Earth Syst. Sci., 20, 3099-3108, 10.5194/hess-20-3099-2016, 2016.

Vavilin, V. A., and Rytov, S. V.: Nitrate denitrification with nitrite or nitrous oxide as intermediate products: Stoichiometry, kinetics and dynamics of stable isotope signatures, Chemosphere, 134, 417-426, 2015.

Vitòria, L., Soler, A., Canals, À., and Otero, N.: Environmental isotopes (N, S, C, O, D) to determine natural attenuation processes in nitrate contaminated waters: Example of Osona (NE Spain), Appl. Geochem., 23, 3597-3611, 2008.

Vogel, J. C., Talma, A. S., and Heaton, T. H. E.: Gaseous nitrogen as evidence for denitrification in groundwater, J. Hydrol., 50, 191-200, 1981.

Wassenaar, L. I.: Evaluation of the origin and fate of nitrate in the Abbotsford Aquifer using the isotopes of ^{15}N and ^{18}O in NO_3^-, Appl. Geochem., 10, 391-405, 1995.

Wassenaar, L. I., Hendry, M. J., and Harrington, N.: Decadal geochemical and isotopic trends for nitrate in a transboundary aquifer and implications for agricultural beneficial management practices, Environ. Sci. Technol., 40, 4626-4632, 2006.

Weil, R. R., Weismiller, R. A., and Turner, R. S.: Nitrate contamination of groundwater under irrigated coastal plain soils, J. Environ. Qual., 19, 1990.

Xu, S., Kang, P., and Sun, Y.: A stable isotope approach and its application for identifying nitrate source and transformation process in water, Environ. Sci. Pollut. Res., 23, 1133-1148, 2015.

Xue, D., Botte, J., De Baets, B., Accoe, F., Nestler, A., Taylor, P., Van Cleemput, O., Berglund, M., and Boeckx, P.: Present limitations and future prospects of stable isotope methods for nitrate source identification in surface- and groundwater, Water Res., 43, 1159-1170, 2009.

Yang, C.-Y., Wu, D.-C., and Chang, C.-C.: Nitrate in drinking water and risk of death from colon cancer in Taiwan, Environ. Int., 33, 649-653, 10.1016/j.envint.2007.01.009, 2007.

Zirkle, K. W., Nolan, B. T., Jones, R. R., Weyer, P. J., Ward, M. H., and Wheeler, D. C.: Assessing the relationship between groundwater nitrate and animal feeding operations in Iowa (USA), Sci. Total Environ., 566–567, 1062-1068, 2016.

Table 1. Details of groundwater monitoring wells and continuous core collection at CFO1 and CFO4 (all screens installed at bottom of the well).

Site	Well/Core hole ID	Type[†]	Lateral distance from EMS* (m)	Ground elevation (m asl)	Total depth (m below ground)	Screen length (m)	Lithology of screened interval	K (m s^{-1})
CFO1	DMW1	WTW	60	869.7	5.0	4.0	Sand	
	DMW2	WTW	10	867.2	6.0	4.0	Sand	1.2×10^{-7}
	DMW3	WTW	2	867.5	3.7	2.0	Sand	
	DMW4	WTW	160		4.2	4	Sand	1.3×10^{-6}
	DMW5	WTW	270	866.4	6.8	4.0	Clayey sand	1.7×10^{-5}
	DMW6	WTW	310		6.7	4		
	DP10-1	Piezo	2	867.8	18.6	0.5	Clay	1.6×10^{-9}
	DP10-2	Piezo	2	867.9	8.0	1.5	Sand	3.6×10^{-5}
	DMW10	WTW	340	868.0	7.2	3.0	Clay	3.0×10^{-7}
	DP11-10b	Piezo	340	868.0	20	0.5	Clay	2.2×10^{-8}
	DMW11	WTW	470	864.8	7.0	3.0	Sand and clay	4.2×10^{-5}
	DP11-11b	Piezo	470		20	0.5	Clay	6.3×10^{-9}
	DMW12	WTW	50	867.6	7.0	3.0	Sand and clay	7.4×10^{-6}
	DP11-12b	Piezo	50	867.6	20.1	1.0	Clay	1.1×10^{-8}
	DMW13	WTW	35	867.1	7.0	3.0	Sand	8.9×10^{-6}
	DP11-13b	Piezo + core	35	867.1	20.0	0.5	Clay	
	DMW14	WTW	105	865.7	7.0	3.0	Clay	5.7×10^{-6}
	DP11-14b	Piezo	105	865.7	20.0	0.5	Sand	1.1×10^{-6}
	DMW15	WTW	185		7.0	3	Clay	2.4×10^{-8}
	DP11-15b	Piezo	185		20.0	0.5	Clay	1.4×10^{-7}
	DMW16	WTW	320	866.0	6.0	3.0	Sand and clay	-
	DP11-16b	Piezo	320		20.0	0.5	Clay	3.2×10^{-9}
	DC15-20	Core	76		15			
	DC15-21	Core	45		10.5			
	DC15-22	Core	22		12			
	DC15-23	Core	9		15			
CFO4	BC1	WTW	110	857.0	6.9	3.1	Clay and sandstone	
	BC2	WTW	365	859.4	7.0	3.1	Clay and sandstone	2.2×10^{-7}
	BC3	WTW	145	858.6	6.8	3.1	Clay and sandstone	1.3×10^{-6}
	BC4	WTW	95	858.8	5.9	3.0	Clay and sandstone	3.4×10^{-6}
	BC5	WTW	105	859.5	7.5	4.5	Clay and sandstone	
	BMW1	WTW	4	858.6	7.1	3.1	Clay and sandstone	4.3×10^{-6}
	BMW2	WTW	3	857.9	7.5	4.5	Clay and sandstone	8.5×10^{-7}
	BMW3	WTW	8	858.6	6.0	3.0	Clay and sandstone	
	BMW4	WTW	14	858.0	7.5	4.8	Clay and sandstone	1.0×10^{-5}
	BMW5	WTW	60	858.0	7.5	4.5	Clay and sandstone	
	BP5-15	Piezo	60	858.1	15.3	1.5	Sandstone	1.0×10^{-7}
	BMW6	WTW	150	856.9	7.5	4.5	Clay and sandstone	4.0×10^{-6}
	BP6-15	Piezo	150	856.8	15.2	1.5	Sandstone	3.0×10^{-6}
	BMW7	WTW	140	856.7	7.5	4.5	Clay and sandstone	1.0×10^{-6}
	BP10-15e	Piezo	4	858.2	14.9	1.5	Sandstone	2.9×10^{-5}
	BP10-15w	Piezo	10	858.0	15.0	1.5	Sandstone	1.0×10^{-5}

*EMS=Earthen manure storage
[†]WTW=water table well, Piezo = piezometer, Core = continuous core

Table 2. Range of measured concentrations of TN, NH$_3$-N, NO$_x$-N (NO$_2$-N + NO$_3$-N) and TON at each study site. At CFO1 results from monitoring well DMW3 are presented separately because values in this well differed substantially from all other wells.

Site	N-pool	TN (mg L^{-1})	NH$_3$-N (mg L^{-1})	NO$_x$-N (mg L^{-1})	TON (mg L^{-1})
CFO1	EMS	550 – 1820	275 – 747	<0.1 – 0.4	73 – 1301
	Catch-basin	200 – 1440	2.5 – 7.3	<0.1	196 – 1437
	DMW3	278 – 548	219 – 479	<0.1 – 50[*]	31.3 – 73.9
	Other monitoring wells	<0.25 – 33.4	<0.05 – 2.9	<0.1 – 31.4[**]	<0.2 –3.7
CF04	EMS^	1000 – 1240	724 – 747	0.25 - 0.29	275 –492
	Monitoring wells	<0.25 – 84.6	<0.05 – 0.23	<0.1 – 80.4	<0.2 –13.9

[*] NO$_x$-N of 50 mg L^{-1} in DMW3 consisted of 12.6 mg L^{-1} as NO$_3$-N and 37.4 mg L^{-1} as NO$_2$-N.
[**] NO$_x$-N max in groundwater measured in core (NO$_3$-N = 66.4 mg L^{-1}, NO$_x$-N = 67.8 mg L^{-1})
^Range across three replicates measured on 25 August 2011

Table 3. Calculated f_d and f_m based on measured Cl$^-$ and NO$_3$-N concentrations and stable isotope values of NO$_3^-$.

Study area	Sample ID*	Cl$^-$ (mg L^{-1})	NO$_3$-N (mg L^{-1})	$\delta^{15}N_{NO3}$ (‰)	$\delta^{18}O_{NO3}$ (‰)	f_d (mean ± stdev)	f_m[**] (mid-range)
CFO1	DP11-13_4.3m	28.5	7.0	30.3	9.8	0.30 ± 0.15	0.58
	DP11-13_5.2m	25.0	7.8	31.0	10.8	0.34 ± 0.13	0.58
	DP11-13_7m	72.3	12.0	31.6	10.2	0.27 ± 0.13	0.65
	DP11-13 _7.9m	70.8	9.1	36.4	14.0	0.17 ± 0.09	0.68
	DP11-13_8.8m	81.7	10.9	29.6	9.9	0.32 ± 0.15	0.63
	DC15-22_10m	73.0	11.0	26.1	7.4	0.47 ± 0.21	0.63
	DP10-2	74.5	11.8	24.2	4.8	0.52 ± 0.22	0.63
	DMW11	436.1	17.1	33.3	10.9	0.17 ± 0.07	0.83
	DMW12	78.0	2.57	29.8	14.3	0.23 ± 0.10	0.54
	DMW13	56.7	23.7	23.0	6.8	0.56 ± 0.22	0.65
	DP11-12b	95.7	0.6	35.9	17.0	0.15 ± 0.08	0.54
CFO4	BC4	163.1	35.1	30.6	1.6	0.37 ± 0.13	0.82
	BMW2	595.6	16.5	41.6	8.3	0.13 ± 0.06	0.92
	BMW5	131.2	12.9	28.9	6.5	0.34 ± 0.16	0.63
	BMW6	156.0	0.4	70.5	22.1	0.01 ± 0.01	0.56
	BMW7	134.7	11.6	34.0	5.9	0.21 ± 0.11	0.68

*central depth of core samples, x, indicated as SampleID_xm.
** maximum f_m is 1 for all samples, which implies no mixing.
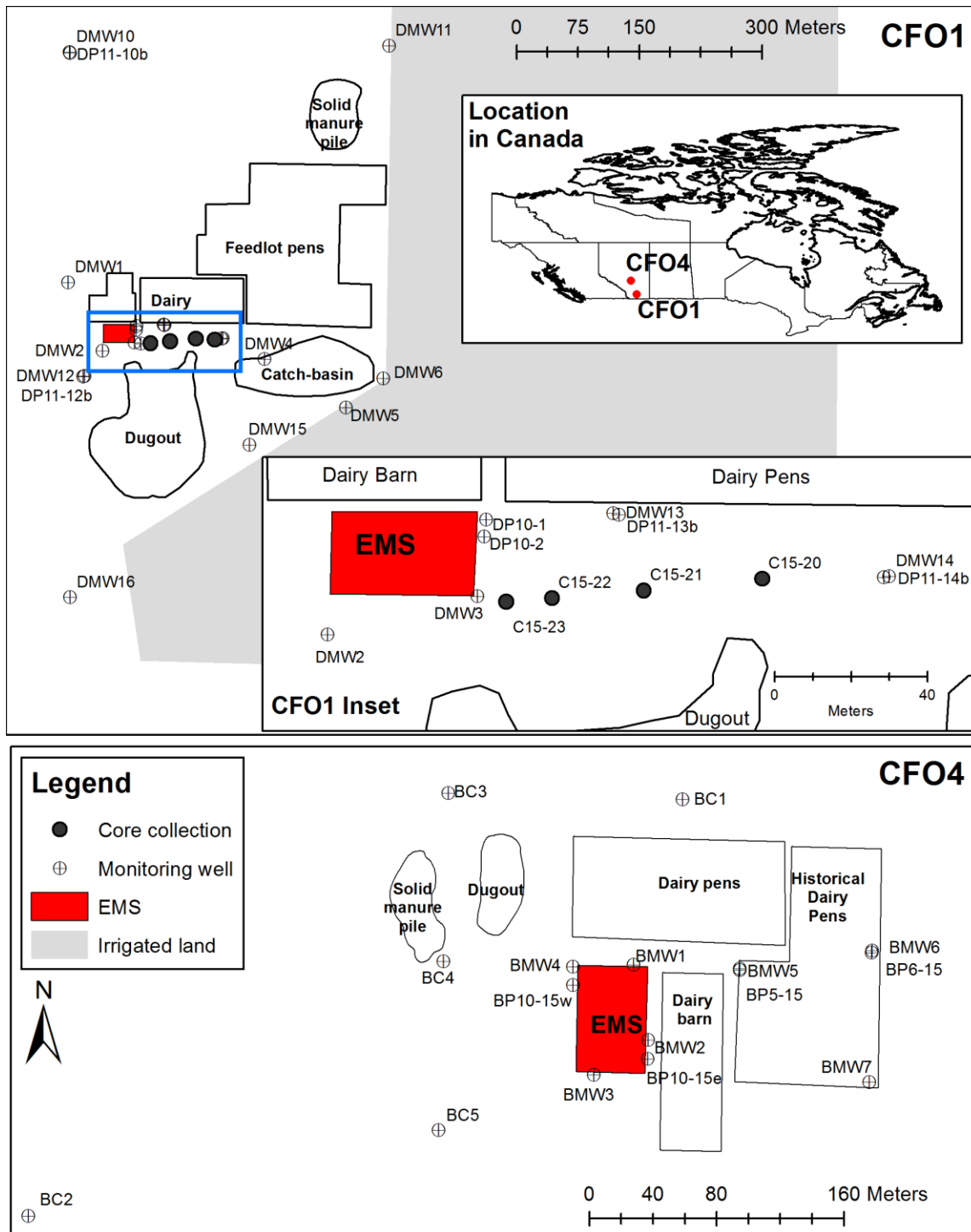
Figure 1: Map of study sites CFO1 and CFO4, showing locations of groundwater monitoring wells, core collection, earthen manure storages (EMS), dairy and feedlot pens, manure piles, and irrigated land. Blue rectangle indicates extent of CFO1 inset.
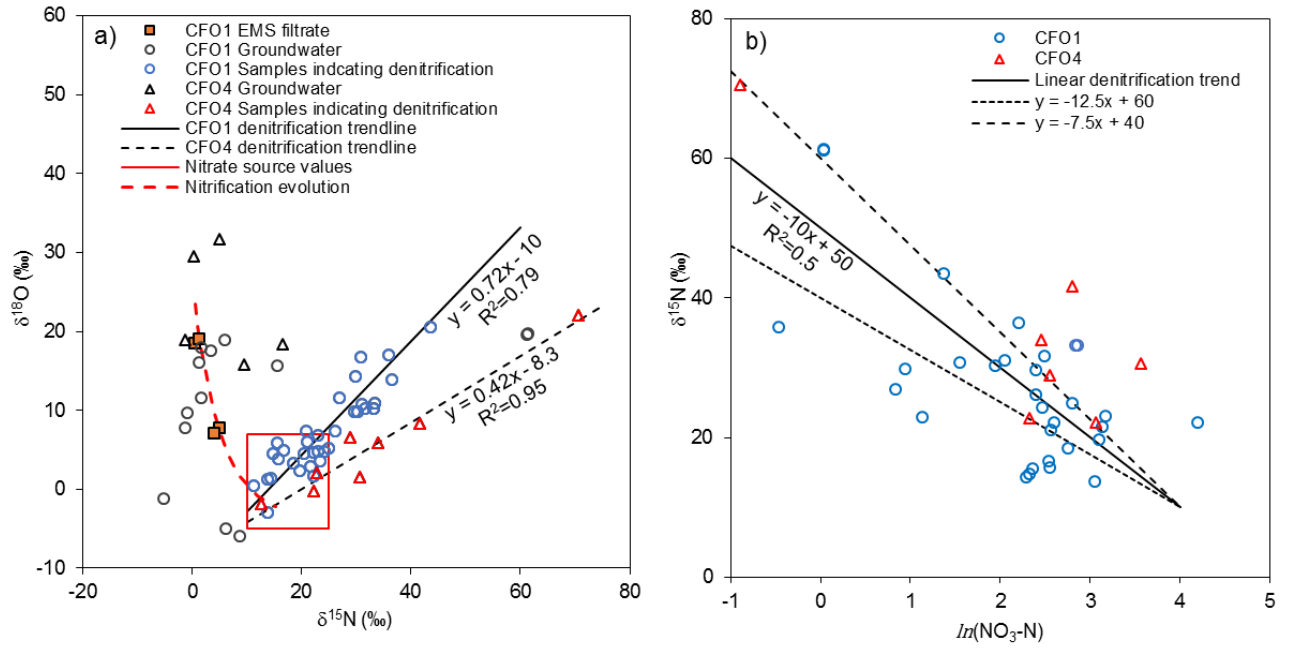
Figure 2 (a) Cross-plot of stable isotopes of nitrate at CFO1 and CFO4 showing hypothetical nitrification trend, boundary of manure-sourced NO_3^- values and linear enrichment trends associated with denitrification, (b) enrichment of $\delta^{15}N_{NO3}$ during denitrification (only samples within source region and with evidence of denitrification are shown) dashed lines represent ±1 std. dev. of enrichment factor (ε = -10) estimated from measured data.
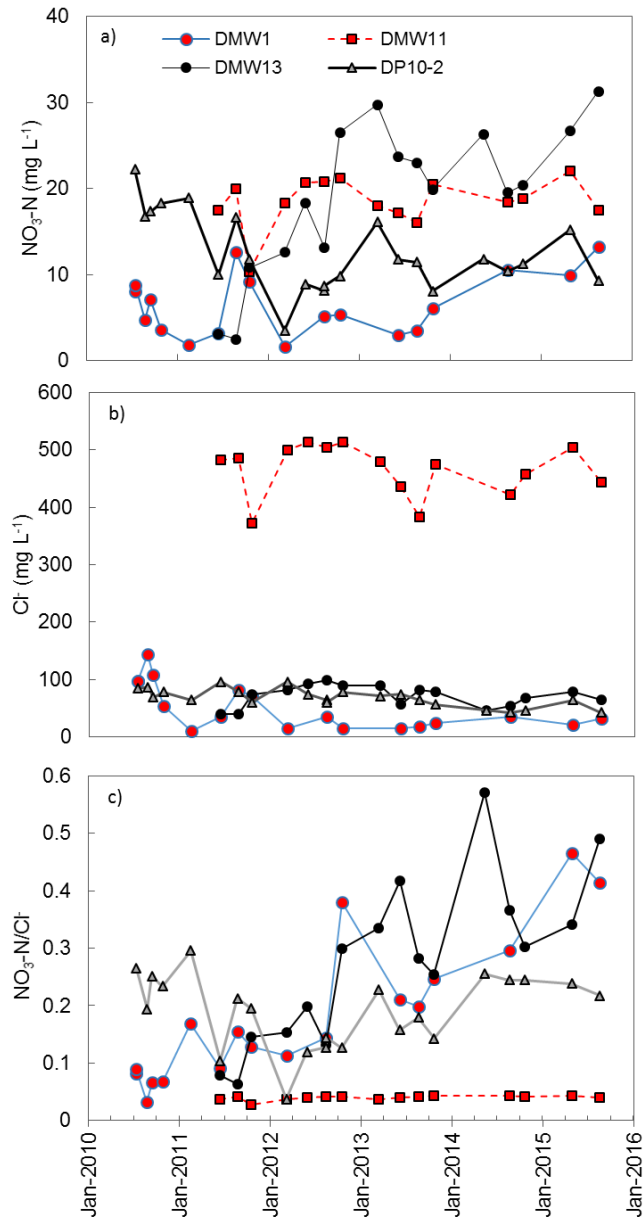
Figure 3 Temporal variations in (a) NO$_3$-N, (b) Cl$^-$, and (c) NO$_3$-N/Cl$^-$ at CFO1. Only wells with NO$_3$-N > 10 mg L^{-1} are shown.
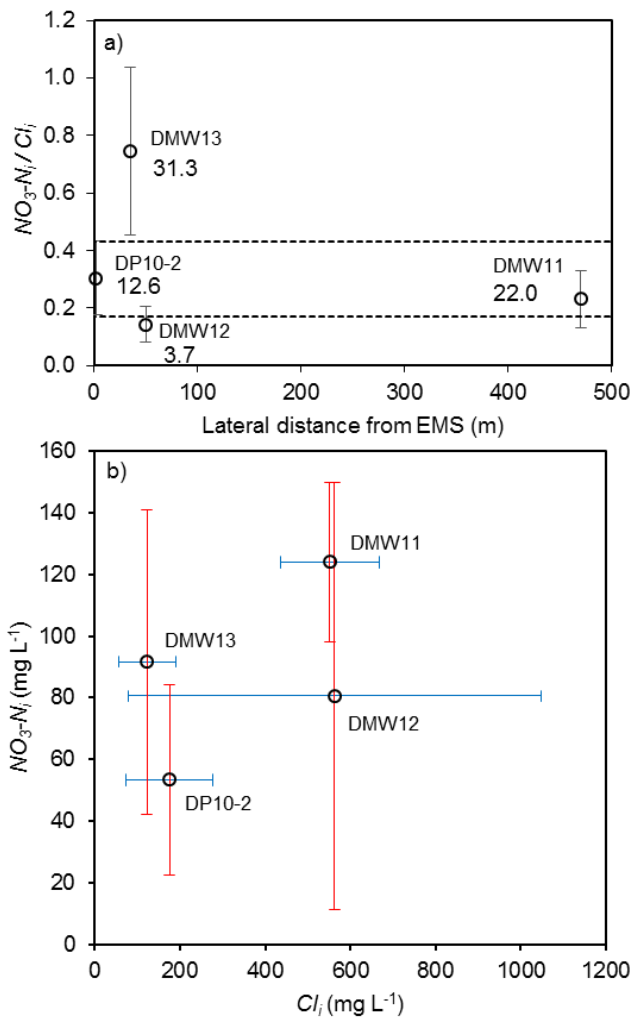
Figure 4 (a) Estimated NO_3-N_i/Cl_i ratios (mean and st. dev.) in water table wells with evidence of denitrification at CFO1, plotted with distance from earthen manure storage (EMS), where dashed lines are the upper and lower bounds of DP10-2 (EMS source) and values are maximum measured NO_3-N (mg L^{-1}). (b) Estimated concentrations of NO_3-N_i and Cl_i at CFO1 (mid-range, error bars are max. and min. values).
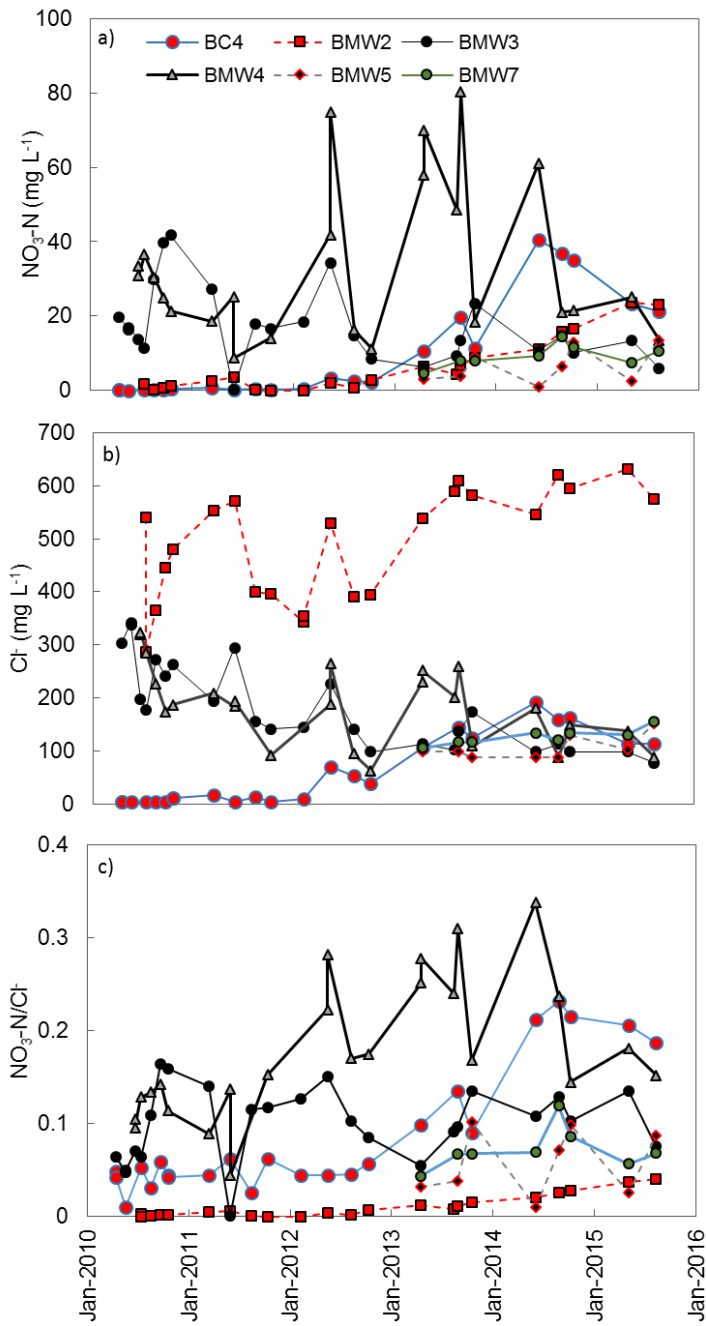
Figure 5 Temporal variations in (a) NO₃-N, (b) Cl⁻, and (c) NO₃-N/Cl⁻ at CFO4. Only wells with NO₃-N > 10 mg L⁻¹ are shown.
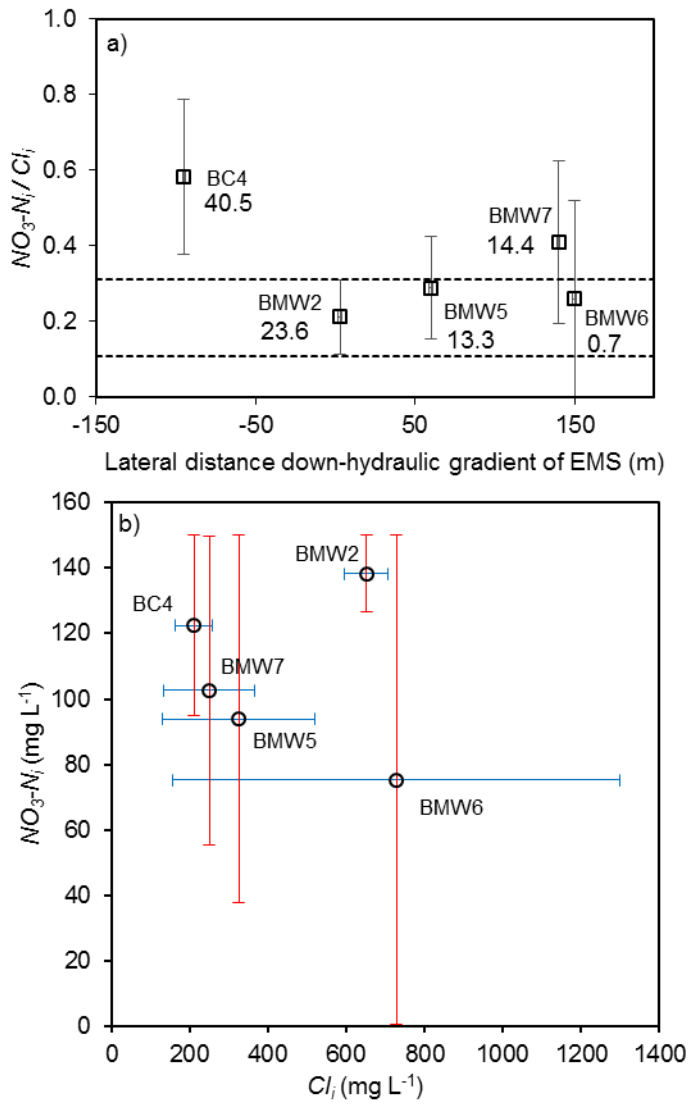
Figure 6 (a) Estimated *NO₃-Nᵢ/Clᵢ* ratios (mean and st. dev.) in water table wells with evidence of denitrification at CFO4, plotted with distance from earthen manure storage (EMS), where dashed lines are upper and lower bounds of BMW2 (EMS source) and values are maximum measured NO₃-N (mg L⁻¹). (b) Estimated concentrations of *NO₃-Nᵢ* and *Clᵢ* at CFO1 (mid-range, error bars are max. and min. values).
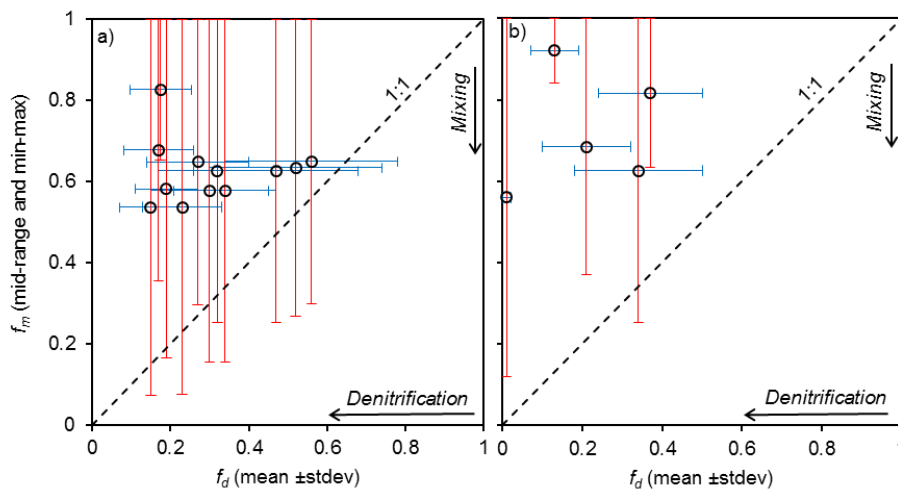
Figure 7 Relative contributions to NO₃⁻ attenuation by mixing and denitrification, as indicated by estimated f_m and f_d at (a) CFO1 and (b) CFO4, for groundwater samples with denitrification indicated by stable isotope values of NO₃⁻.
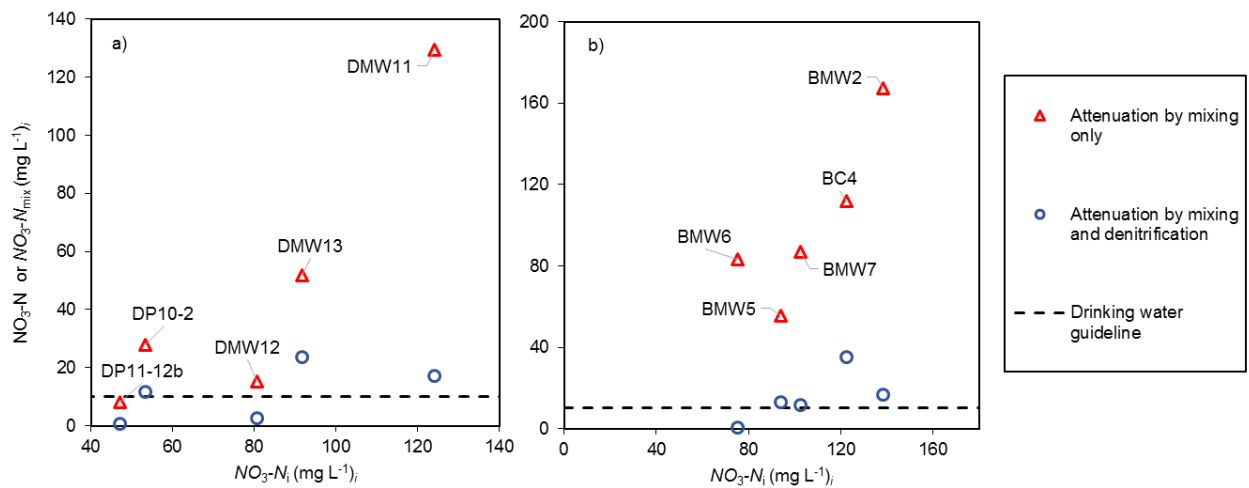
Figure 8 Measured concentrations of NO₃-N (blue circles - attenuation by mixing and denitrification) and NO_3-N_{mix} (red triangles - attenuation by mixing only) vs mid-range estimate of NO₃-N$_i$ at a) CFO1 and b) CFO4. Dashed lines are drinking water guideline (10 mg L⁻¹ of NO₃-N).
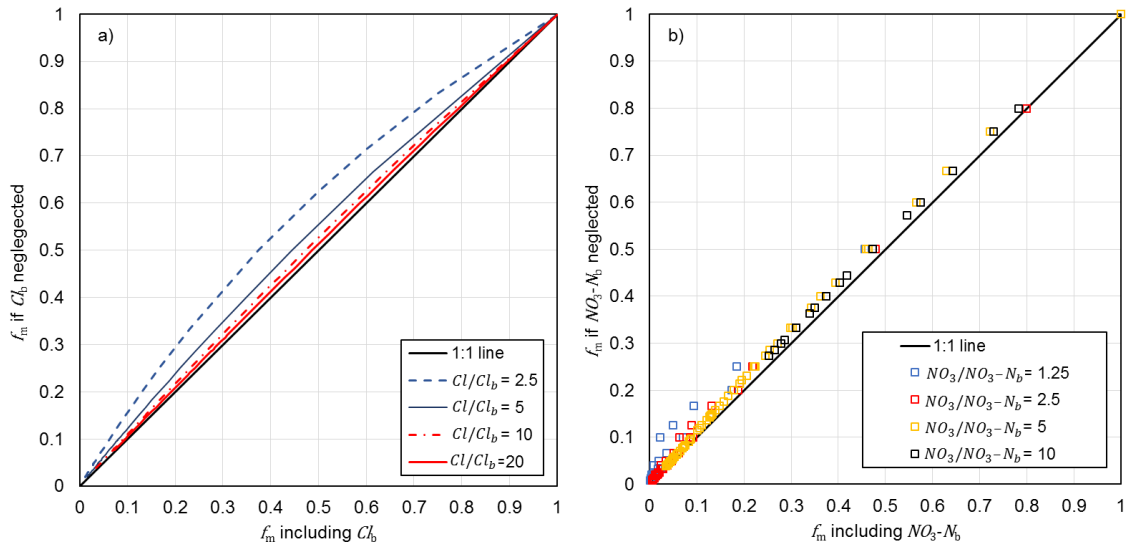
Figure 9 Effect of neglecting background concentrations (Cl_b or NO_3-N_b) in the mixing model on calculated f_m over the range of values in this study.